

1 **First-order visual interneurons distribute distinct contrast and luminance**
2 **information across ON and OFF pathways to achieve stable behavior**

3

4

5 Madhura Ketkar^{*1,2}, Burak Gür^{*1,2}, Sebastian Molina-Obando^{*1,2}, Maria Ioannidou^{1,3},
6 Carlotta Martelli¹ and Marion Silies¹

7

8

9

10 ¹ Institute of Developmental Biology and Neurobiology, Johannes-Gutenberg University Mainz,
11 55128 Mainz, Germany.

12 ² Göttingen Graduate School for Neurosciences, Biophysics, and Molecular Biosciences (GGNB)
13 and International Max Planck Research School (IMPRS) for Neurosciences at the University of
14 Göttingen, 37077 Göttingen, Germany

15 ^{1,3} Present address: School of Physics, Faculty of Sciences, Aristotle University of Thessaloniki,
16 54124, Greece

17 * these authors contributed equally to this work

18

19

20

21 Corresponding author: msilies@uni-mainz.de

22 **Abstract**

23

24 The accurate processing of contrast is the basis for all visually guided behaviors. Visual scenes
25 with rapidly changing illumination challenge contrast computation, because adaptation is not fast
26 enough to compensate for such changes. Yet, human perception of contrast is stable even when
27 the visual environment is quickly changing. The fruit fly *Drosophila* also shows nearly luminance
28 invariant behavior for both ON and OFF stimuli. To achieve this, first-order interneurons L1, L2
29 and L3 all encode contrast and luminance differently, and distribute information across both ON
30 and OFF contrast-selective pathways. Behavioral responses to both ON and OFF stimuli rely on
31 a luminance-based correction provided by L1 and L3, wherein L1 supports contrast computation
32 linearly, and L3 non-linearly amplifies dim stimuli. Therefore, L1, L2 and L3 are not distinct inputs
33 to ON and OFF pathways but the lamina serves as a separate processing layer that distributes
34 distinct luminance and contrast information across ON and OFF pathways to support behavioral
35 performance in varying conditions.

36 **Introduction**

37
38 Across species, contrast information forms the basis of visual computations. For our perception
39 to be stable, our eyes must compute contrast relative to the mean illumination of a scene. In
40 natural environments, illumination changes by several orders of magnitude not only from dawn to
41 dusk, but also at much faster timescales as our eyes saccade across a scene or we quickly move
42 from sun to shade (Frazor and Geisler, 2006; Mante et al., 2005; Rieke and Rudd, 2009). Thus,
43 the computation of contrast needs to be invariant to rapid changes in luminance, such that visual
44 perception of a given contrast remains constant. This is accomplished by human perception, and
45 neuronal responses in the cat lateral geniculate nucleus (LGN) display contrast constancy at rapid
46 time scales (Burkhardt et al., 1984; Mante et al., 2005). However, contrast encoding in
47 photoreceptors is not luminance invariant when the stimulus changes more rapidly than
48 photoreceptor adaptation (Laughlin and Hardie, 1978; Normann and Werblin, 1974).

49
50 The visual OFF pathway in fruit flies, sensitive to contrast decrements, also displays contrast-
51 constant behavior (Ketkar et al., 2020), allowing to investigate the underlying mechanisms. In the
52 OFF pathway, luminance information itself is maintained postsynaptic to photoreceptors, and is
53 crucial for the accurate estimation of contrast, resulting in contrast-constant behavior. Luminance
54 serves as a corrective signal that scales contrast computation when background luminance
55 quickly changes (Ketkar et al., 2020). The requirement of such a corrective signal can be
56 theoretically expected regardless of ON and OFF contrast polarities, since the adaptational
57 constraints in dynamic environments challenge both contrast polarities. However, the ON and
58 OFF pathways are not mere sign-inverted versions of each other since they face different
59 environmental challenges (Clark et al., 2014; Ruderman, 1994) and have evolved several
60 structural and physiological asymmetries (Chichilnisky and Kalmar, 2002; Jin et al., 2011;
61 Leonhardt et al., 2016; Ratliff et al., 2010). It is thus not clear if this luminance invariance is a
62 general feature of all visual pathways, and how luminance and contrast information are distributed
63 across visual pathways to establish contrast constancy is not known.

64
65 *Drosophila melanogaster* offers a promising model system to study the pathway-specific function
66 of luminance since the ON and OFF motion pathways have been well characterized on the
67 cellular, circuit and behavioral levels (Behnia et al., 2014; Yang and Clandinin, 2018). In the fly
68 visual system, neurons were assigned to distinct ON or OFF pathways based on physiological
69 properties (Molina-Obando et al., 2019; Serbe et al., 2016; Shinomiya et al., 2019; Silies et al.,
70 2013; Strother et al., 2017), anatomical connectivity (Shinomiya et al., 2014; Takemura et al.,
71 2015, 2013, 2017), and behavioral function (Clark et al., 2011; Silies et al., 2013). ON and OFF
72 contrast selectivity first arises two synapses downstream of photoreceptors, in medulla neurons
73 (Fischbach and Dittrich, 1989; Serbe et al., 2016; Silies et al., 2013; Strother et al., 2017; Yang
74 et al., 2016). They receive photoreceptor information through the lamina neurons L1-L3, which
75 project to specific medulla layers (Meinertzhagen and O'Neil, 1991; Strother et al., 2014).
76 Although L1-L3 all show the same response polarity, and hyperpolarize to light onset and
77 depolarize to light offset, L1 projects to layers where it mostly connects to ON-selective medulla
78 neurons. Similarly, L2 and L3 project to layers where OFF-selective medulla neurons get most of
79 their inputs (Shinomiya et al., 2014; Takemura et al., 2015, 2013). L1 is thus thought to be the

80 sole major input of the ON pathway, whereas L2 and L3 are considered the two major inputs of
81 the OFF pathway (Figure 1A) (Clark et al., 2011; Joesch et al., 2008; Shinomiya et al., 2019).
82 Among these, L2 is contrast-sensitive, but cannot support contrast constancy alone if
83 photoreceptor adaptation is insufficient. Instead, contrast constancy in OFF-motion guided
84 behavior is ensured by a corrective signal from luminance-sensitive L3 neurons (Ketkar et al.,
85 2020). It is not known whether ON-motion driven behavior also requires luminance information
86 and whether L1 can provide it along with its contrast signal (Figure 1B).

87 Contrast and luminance are both encoded by the transient and sustained response components
88 in both vertebrates and invertebrate photoreceptors (Laughlin and Hardie, 1978; Normann and
89 Perlman, 1979; Normann and Werblin, 1974; Shapley and Enroth-Cugell, 1984), which are
90 captured differentially by their downstream neurons. In the vertebrate retina, many different types
91 of first order interneurons, bipolar cells, exist. Although they are generally thought to capture the
92 contrast component of the photoreceptors response, luminance information has been shown to
93 be preserved in post-photoreceptor visual circuitry post of the retina (Awatramani and Slaughter,
94 2000; Ichinose and Hellmer, 2016; Ichinose and Lukasiewicz, 2007; Odermatt et al., 2012; Oesch
95 and Diamond, 2011). As suggested by their sustained response component, different degrees of
96 luminance-sensitivity exists across bipolar cell types (Baden et al., 2016; Euler et al., 2014).
97 Furthermore, ON and OFF contrast selectivity emerges at the bipolar cell layer, where ON
98 selectivity emerges through glutamatergic inhibition (Masu et al., 1995). These ON and OFF
99 bipolar cells also split anatomically, as they innervate different layers (Euler et al., 2014).
100 Together, many parallels exist between the *Drosophila* visual system and the vertebrate retina,
101 including the response properties of photoreceptors, the layered organization and the existence
102 of ON and OFF pathways (Clark and Demb, 2016; Mauss et al., 2017). However, in contrast to
103 the vertebrate retina, fewer first order interneuron types distribute contrast and luminance
104 information, and contrast selectivity itself clearly only occurs one synapse further downstream,
105 where neurons postsynaptic to lamina neurons are either ON or OFF selective. Comparing the
106 vertebrate retina with the insect visual system, it is unclear how just three first order interneurons
107 distribute their different physiological properties across visual pathways.
108

109 Here, we show that luminance and contrast information is distributed to, and is of behavioral
110 relevance for both ON and OFF pathways. *In vivo* calcium imaging experiments reveal that each
111 first order interneuron is unique in its contrast and luminance encoding properties. Whereas L2 is
112 purely contrast sensitive, L1 encodes both contrast and luminance in distinct response
113 components. L1 linearly scales with luminance, whereas the luminance-sensitive L3 non-linearly
114 amplifies dim light. Behavioral experiments further show that these differential luminance- and
115 contrast- encoding properties translate into distinct behavioral roles. In the ON pathway, L1 and
116 L3 both provide luminance information for higher luminance invariance than possible by the
117 contrast input alone. Furthermore, L2, known as the OFF-pathway contrast input, provides
118 contrast information to the ON-pathway, in addition to L1. Surprisingly, both L1 and L3 neurons
119 are necessary and sufficient for OFF behavior. These findings indicate that L1, L2, and L3 do not
120 constitute ON- or OFF-specific inputs. Instead, the three first-order interneurons encode
121 luminance and contrast differentially and contribute to computations in both ON and OFF
122 pathways. Together, our data reveal how luminance and contrast information are distributed to

123 both ON and OFF pathways to approach luminance invariance, a core computation of visual
124 systems.

125

126

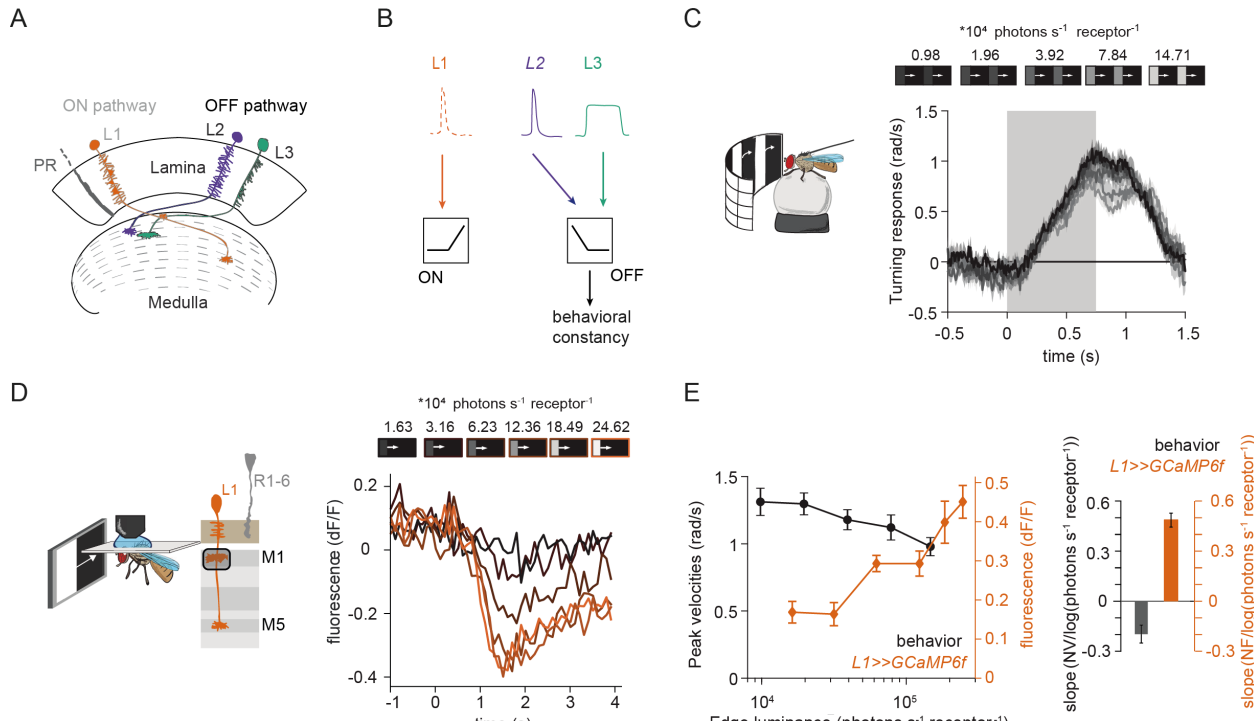
127 **Results**

128 **L1 responses to contrast do not explain ON behavior**

129 Luminance-invariant behavioral responses have been observed in multiple species (Burkhardt et
130 al., 1984; Silies et al., 2014), highlighting their ethological relevance. In *Drosophila*, luminance-
131 invariant behavior has been shown in response to OFF stimuli, where a dedicated luminance-
132 sensitive pathway scales contrast-sensitive inputs to achieve luminance invariance in behavior
133 (Ketkar et al., 2020). The ON pathway is thought to have just one prominent input, L1. We thus
134 asked if luminance invariance is achieved in the ON pathway and if the contrast-sensitive input
135 L1 can explain such invariance. For this purpose, we compared turning behavior of walking flies
136 with the responses of L1. Behavioral responses were measured in a fly-on-a-ball assay. Flies
137 were shown moving ON edges of different luminance but the same 100% Michelson contrast. Fly
138 turning responses were highly similar across luminances, with low-luminance edges eliciting
139 slightly larger turning responses than brighter edges (Figure 1C).

140

141 We wondered if the sole ON pathway input L1 can directly drive this behavior. To test this, we
142 examined the contrast responses of L1 to moving ON edges with comparable parameters and
143 overlapping luminance values as those used in the behavioral assay (Figure 1D). We recorded
144 L1 *in vivo* calcium responses to visual stimuli from its axon terminals expressing GCaMP6f using
145 two-photon microscopy. As described previously, L1 responded negatively to contrast
146 increments, in line with the inverted response polarity of lamina neurons (Figure 1D) (Clark et al.,
147 2011; Laughlin and Hardie, 1978; Yang et al., 2016). The absolute response amplitude of the L1
148 calcium signals scaled with luminance and did not co-vary with the behavioral response (Figure
149 1E). We performed linear regression across calcium signals at different luminances and quantified
150 the slope to extract the luminance dependency of the responses. L1 signals and behavioral
151 responses had opposite luminance dependencies (Figure 1E). Thus, the observed behavior,
152 approaching luminance invariance, cannot be explained solely by contrast inputs from L1,
153 suggesting that the ON-pathway additionally gets luminance-sensitive input.



154

155 **Figure 1: L1 responses to contrast do not explain ON behavior across luminance.** (A) Schematic of lamina
 156 neurons projecting from the lamina to the medulla . L1 is considered the main input to the ON-pathway, whereas L2
 157 and L3 are thought to provide input to the OFF pathway. (B) Transient L2 and sustained L3 neurons provide contrast
 158 and luminance information, respectively, to the OFF pathway to guide contrast-constant behavior (Ketkar et al., 2020).
 159 L1 is thought to have physiological properties very similar to L2 (Clark et al., 2011) and provides contrast information
 160 to the ON selective pathway. (C) Turning response to multiple moving ON edges, displayed on an LED arena that
 161 surrounds a fly walking on an air-cushioned ball. The edge luminance takes five different values, and the background
 162 is dark (~0 luminance), all resulting in 100% contrast. Turning responses are color-coded according to the edge
 163 luminance. The gray box indicates motion duration. n = 10 flies. (D) *In vivo* calcium signals of L1 axon terminal in
 164 medulla layer M1 in response to moving ON edges of six different luminances. Calcium responses of single L1 axon
 165 terminal are shown. (E) Left: Absolute step responses of L1 are plotted together with peak turning velocities calculated
 166 from (C). Behavioral and calcium traces are aligned by maximum response. Right, slope quantification of luminance
 167 dependency for normalized behavior and L1 fluorescence signals. NV = normalized peak velocity, NF = normalized
 168 fluorescent signal. Traces and plots in C and E show mean ± SEM.

169

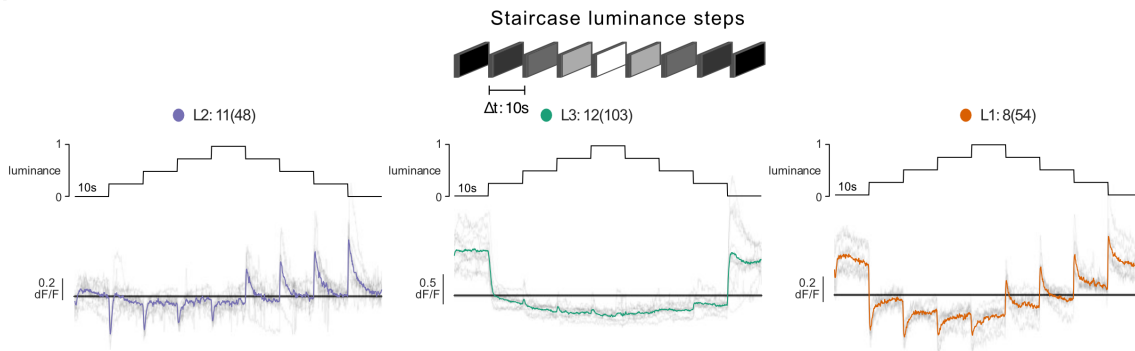
170

171 L1 neuronal responses carry a luminance-sensitive component

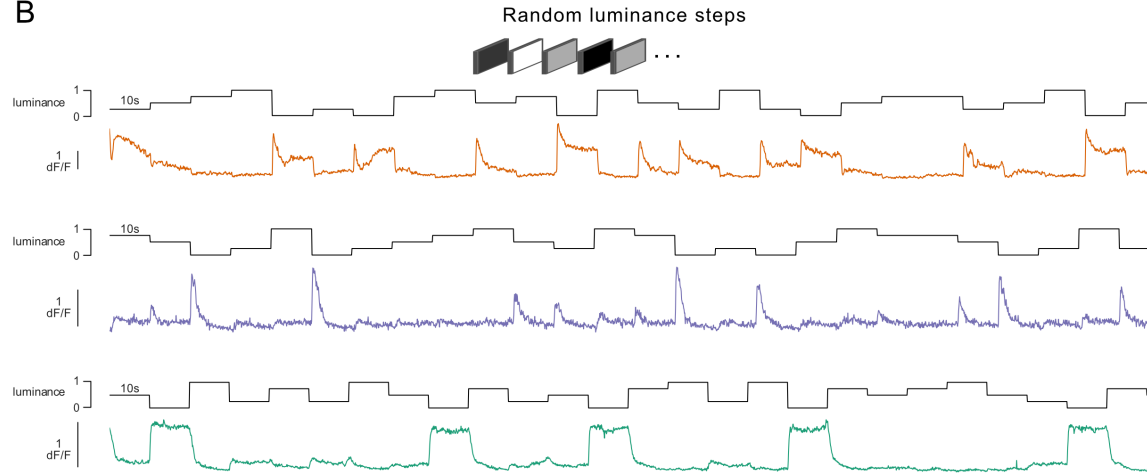
172 To explore the sources of luminance information in first-order interneurons, we measured calcium
 173 signals in L1, L2 and L3. Flies were shown a staircase stimulus with luminance going sequentially
 174 up and down. L1 and L2 showed positive and negative transient responses when luminance
 175 stepped down and up, respectively (Figure 2A), consistent with their contrast sensitivity (Clark et
 176 al., 2011; Silies et al., 2013). L2 did not show any sustained component. L3 showed sustained
 177 responses to OFF steps and was non-linearly tuned to stimulus luminance, responding strongly
 178 to the darkest stimulus. Intriguingly, L1 showed a transient component followed by a sustained
 179 component, suggesting that it encodes luminance in addition to contrast (Figure 2A). The
 180 sustained components of L1 response were negatively correlated with luminance, such that the
 181 baseline calcium signal at each step sequentially increased with decreasing stimulus luminance.

183 Thus, in addition to L3, L1 also maintains luminance information postsynaptically to
 184 photoreceptors.

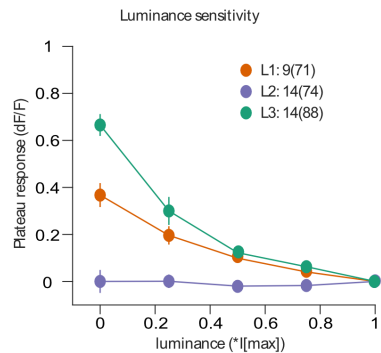
A



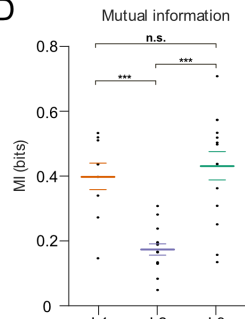
B



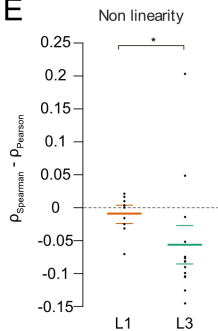
C



D



E

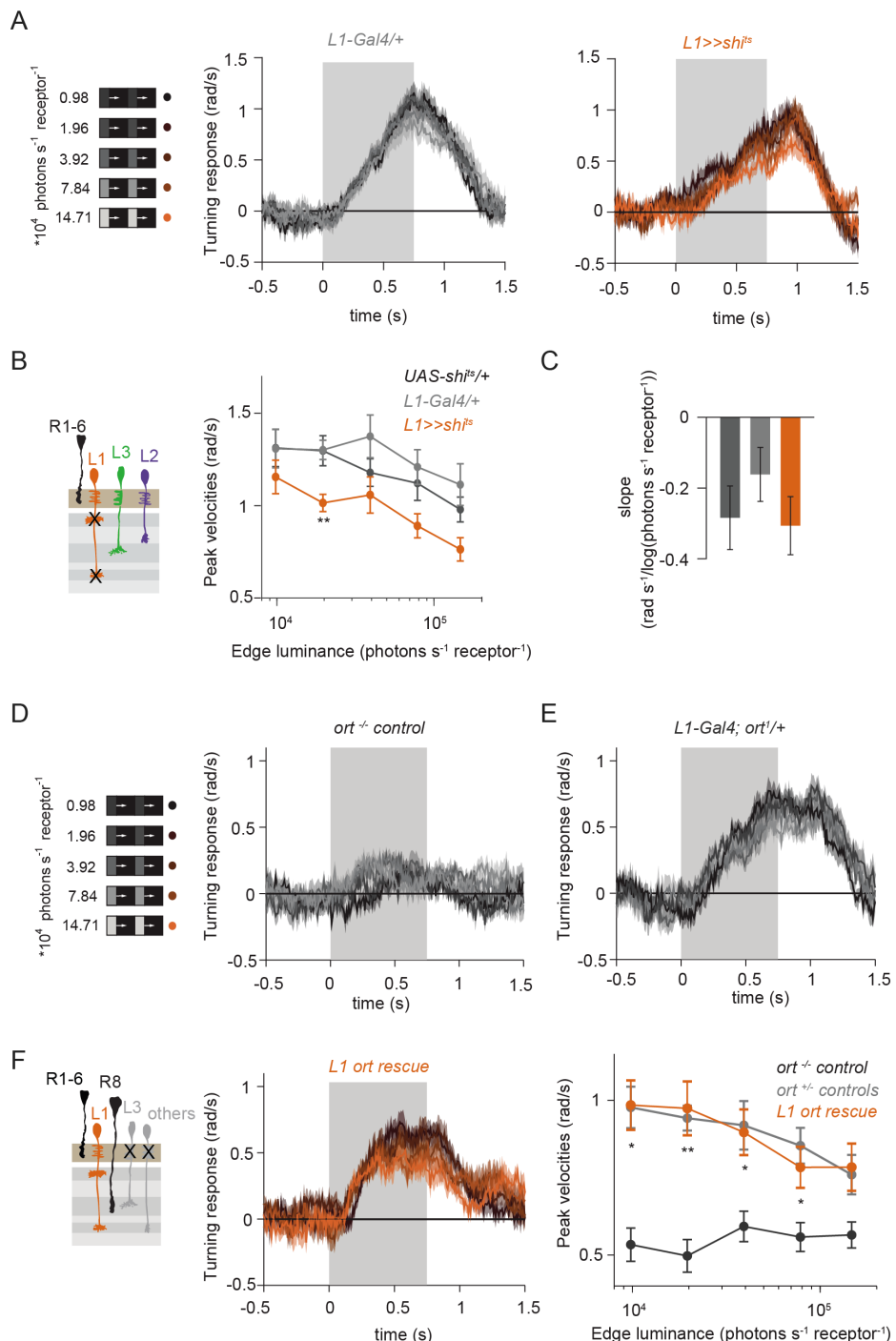


185
 186 **Figure 2: Lamina neuron types L1-L3 are differently sensitive to contrast and luminance.** (A) Schematic of the
 187 'staircase' stimulus. Luminance sequentially steps up through five values and then sequentially steps down. Shown
 188 below are the plateau calcium responses of L1 (orange), L2 (purple) and L3 (green) axon terminals, plotted against
 189 luminance. Colored traces show the mean response, grey traces show individual fly means. (B) Example calcium
 190 traces of single L1, L2 and L3 axon terminals to a stimulus comprising 10 s full-field flashes varying randomly between
 191 five different luminances. (C) Plateau responses of the three neuron types, quantified from the responses to the stimulus
 192 in (B). (D) Mutual information between luminance and calcium signal, ***p < 0.001, one-way ANOVA followed by
 193 multiple comparison test corrected with Bonferroni. (E) Non-linearity quantification of luminance-dependent signals of
 194 L1 and L3 in (C), *p < 0.05, tested by a wilcoxon rank sum test.

195 To explicitly compare luminance information across the three input neurons, we measured
196 responses to randomized luminance and calculated the mutual information between stimulus and
197 the sustained response component (Figure 2B-D). As for the staircase stimulus, L2 transient
198 responses returned to baseline within the 10s of the stimulus presentation, whereas both L1 and
199 L3 displayed sustained components that varied with luminance (Figure 2B,C). Sustained
200 response components in L1 and L3 carried similar mutual information with luminance, and both
201 were higher than L2 (Figure 2D). Interestingly, the luminance-sensitive response components of
202 L1 and L3 scaled differently with luminance. We quantified non-linearity using the difference of
203 Pearson's linear and Spearman's correlation between response and luminance. This value will
204 approach zero if the relationship is linear and increase or decrease if non-linear, depending on
205 the sign of correlation between luminance and response. L1 responses were more linear with
206 respect to luminance than L3 responses, which selectively amplified low luminance (Figure 2E).
207 Thus, the two luminance-sensitive neurons carry different types of luminance information.
208

209 **L1 is not required but sufficient for ON behavior across luminances**

210 Since the canonical ON pathway input L1 is also found to carry luminance information, we
211 hypothesized that it plays a role in mediating the observed behavior. To test this, we silenced L1
212 outputs while measuring ON behavior using *Shibire^{ts}* (Kitamoto, 2001). Silencing L1 severely
213 reduced turning responses when different ON contrasts were interleaved, consistent with previous
214 behavioral studies that identified L1 as the major input to the ON pathway (Clark et al., 2011;
215 Silies et al., 2013) (Supp. Figure 1A-D). However, L1 silencing had little effect on responses to
216 100% contrast at varying luminance, suggesting the existence of other ON pathway inputs (Figure
217 3A,B). To explicitly test if and how L1 silencing changed the luminance dependence of behavioral
218 responses, we quantified the slope of peak turning velocities across different background
219 luminances (Figure 3C). The slopes were slightly negative for both the control and L1-silenced
220 conditions, and did not differ significantly between conditions, suggesting another luminance input
221 masking the L1 contribution. To test this possibility, we asked if L1 is sufficient for ON behavior in
222 dynamically changing luminance conditions. We measured behavioral responses after
223 functionally isolating L1 from other circuitry downstream of photoreceptors. To achieve this, we
224 selectively rescued expression of the histamine-gated chloride channel *Ort* in *ort*-mutant flies,
225 which otherwise lack communication between photoreceptors and their postsynaptic neurons.
226 Behavioral responses of *ort* mutant control flies were absent, indicating that ON-motion behavior
227 fully depends on *Ort* (Figure 3D). Heterozygous *ort* controls turned with the moving 100% contrast
228 ON edges at all luminances (Figure 3E). Flies in which *ort* expression was rescued in L1
229 responded to ON motion at all luminances, and indistinguishable from controls (Figure 3F),
230 showing that L1 can mediate normal turning behavior to ON edges at all luminances. This data
231 confirms L1's general importance in the ON pathway and additionally highlights its behaviorally
232 relevant role of its luminance-sensitive component.



244 **L1 and L3 together provide luminance signals required for ON behavior**

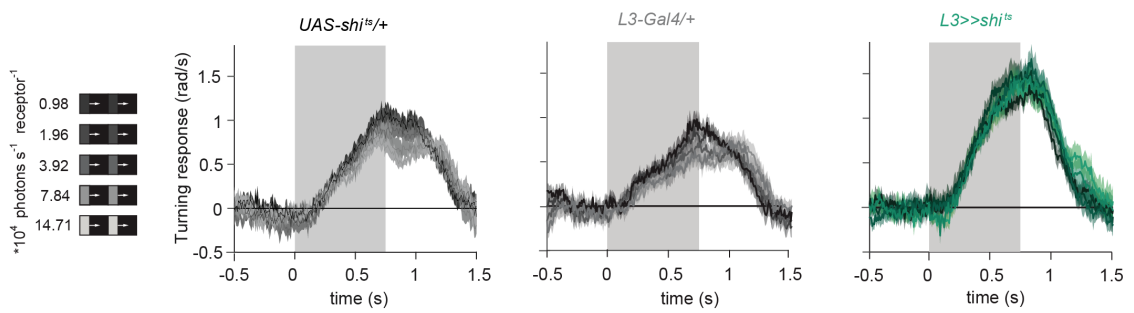
245

246 Our data suggest the existence of a second luminance input to the ON-pathway. In the OFF
247 pathway, the luminance-sensitive L3 neuron provides the necessary luminance-based correction
248 to achieve contrast constancy (Ketkar et al., 2020). Connectomics data suggest that L3 could
249 provide input to the ON pathway as well (Takemura et al., 2013). To test the hypothesis that L3
250 also provides a luminance signal to approach luminance-invariant ON responses, we measured
251 behavioral responses to a set of 100% contrast ON edges at five different luminances while
252 silencing L3 synaptic outputs (Figure 4A,B). Interestingly, unlike controls, L3-silenced flies
253 responded stronger to all ON edges, revealing an unexplored, inhibitory role of L3. However, the
254 responses of L3-silenced flies were still highly similar across luminances. This demonstrates that,
255 like L1, L3 is not alone required for the near-invariant ON pathway behavior. Unlike controls, L3
256 silenced flies did not show a slight increase in turning amplitude at lower edge luminance, also
257 reflected in the differences in their slopes (Figure 4C), suggesting that L3 inputs to the ON
258 pathway also contribute to behavior in a luminance-dependent manner. To further explore this,
259 we next asked if L3 is sufficient for ON behavior and functionally isolated L3 from other circuitry.
260 L3 rescue flies turned to ON edges at all luminances tested (Figure 4D) and significantly rescued
261 turning behavior at low luminances compared to *ort* mutant flies (Figure 4E), showing that L3 is
262 sufficient for ON behavior at low luminances. This further reflects L3's nonlinear preference for
263 dim light seen at the physiological level (Ketkar et al., 2020), (Figure 2C).

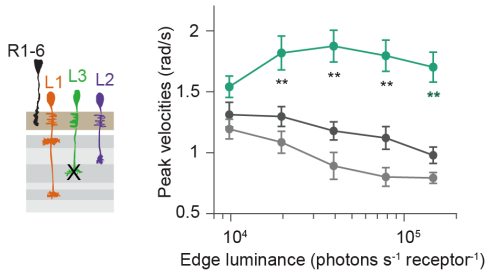
264

265 We found that L3 is a second luminance input to the ON-pathway that, together with L1, supports
266 luminance-invariant responses in ON behavior. To test this, we silenced the outputs of both L1
267 and L3 simultaneously while measuring ON behavior across luminance. Flies still turned to the
268 moving ON edges. However, turning responses of flies lacking both L1 and L3 functional outputs
269 were no longer luminance invariant and turned less than controls in a luminance-dependent
270 manner (Figure 4F,G). Intriguingly, behavioral responses now scaled positively with the edge
271 luminance (Figure 4H), qualitatively recapitulating the LMC contrast-sensitive responses. Thus,
272 L1 and L3 can together account for the luminance information available to the ON pathway. To
273 analyze the extent of the individual contributions of L1 and L3, we compared L1 and L3 *ort* rescues
274 by computing rescue efficiency, defined as the fraction of the difference between positive and
275 negative control behaviors. Whereas L1 fully rescued turning behavior to ON edges at all
276 luminances, L3 significantly rescued turning behavior selectively at low luminances (Figure 4I).
277 Taken together, L1 and L3 both provide distinct types of luminance information to the ON pathway
278 (Figure 4J). Because flies lacking both of these neurons still respond to ON contrast, our data
279 suggest the existence of an unidentified contrast input.

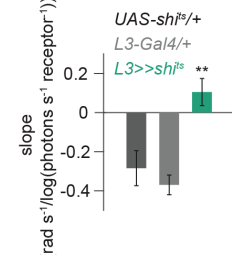
A



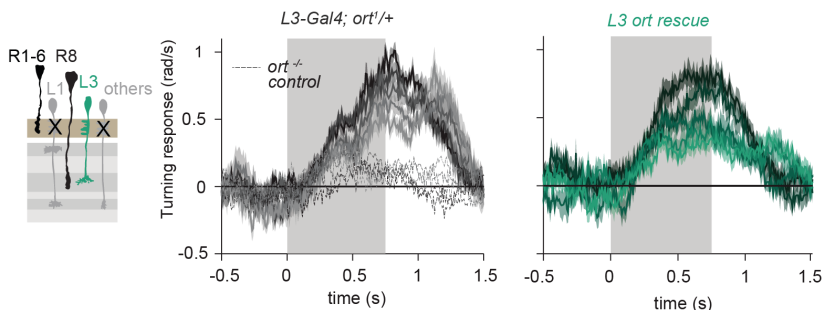
B



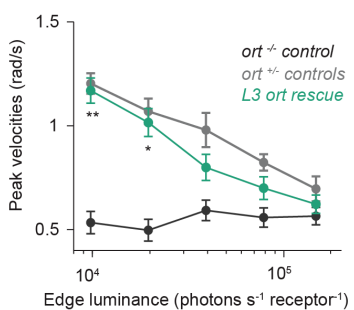
C



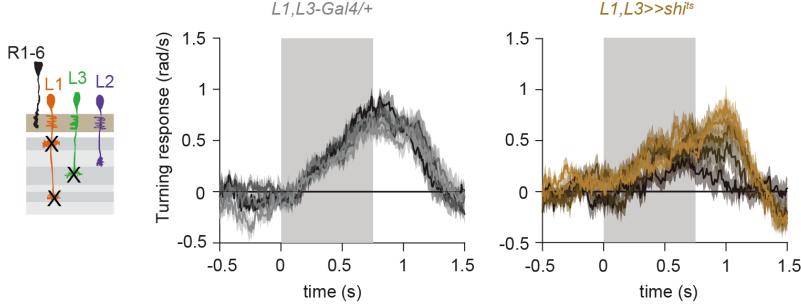
D



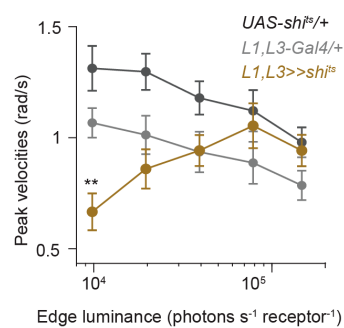
E



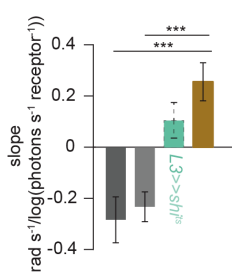
F



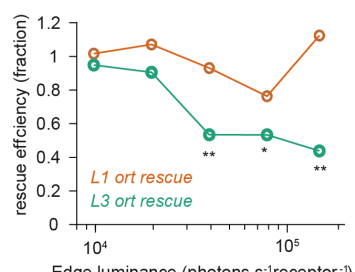
G



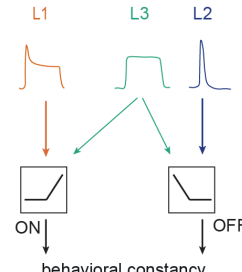
H



I



J

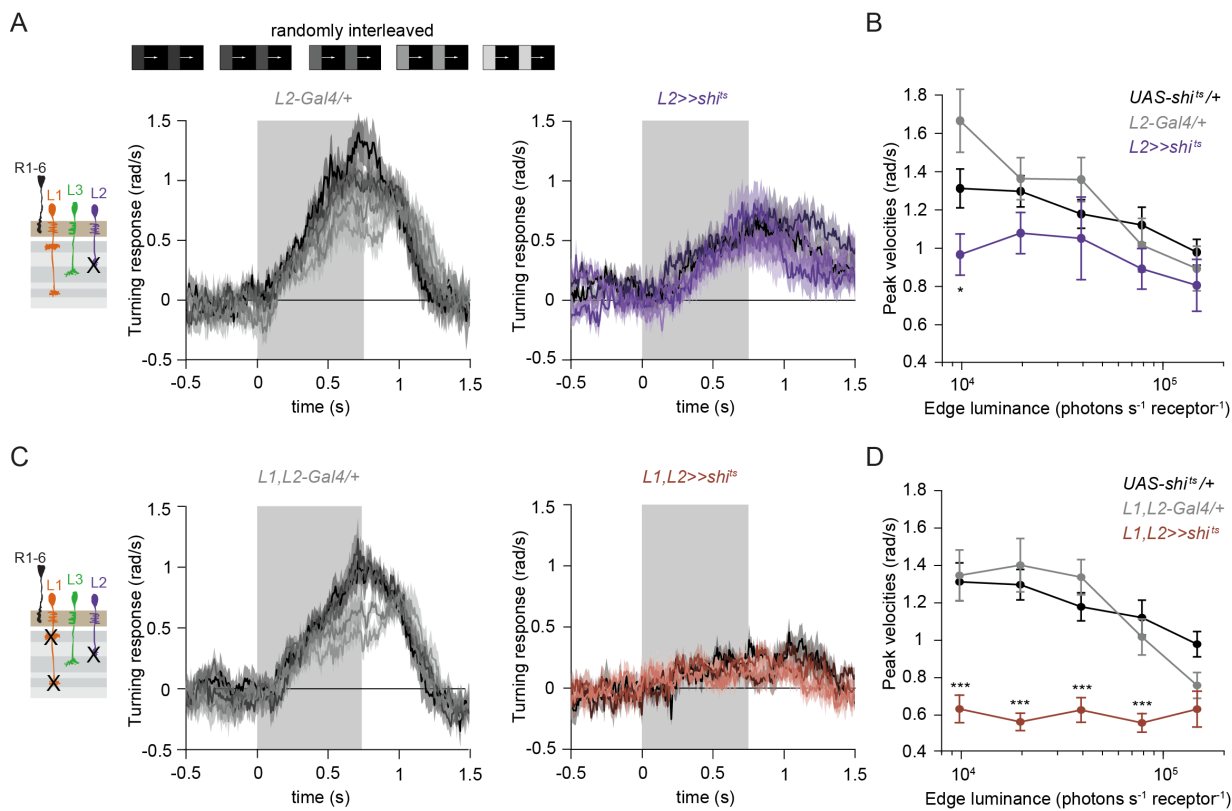


281 **Figure 4: L1 and L3 together provide luminance signals required for ON behavior.** (A) Turning velocities of the
282 controls (gray) and L3-silenced flies (green) in response to five moving ON edges of 100% contrast . The gray box
283 region indicates motion duration. (B) Peak turning velocities for five ON edges quantified during the motion period, **p
284 < 0.01, two-tailed Student's t tests against both controls. (C) Relationship of the peak velocities with luminance,
285 quantified as slopes of the linear fits to the data in (B). Fitting was done for individual flies. Sample sizes are n = 10
286 (*UAS-shi^{is}/+,L3>>shi^{is}*) and n = 8 (*L3⁰⁵⁹⁵-Gal4/+*). (D) Schematic of the L3 *ort* rescue genotype and turning responses
287 of the heterozygous control (gray) and rescue (green) flies. (E) Peak turning velocities, *p<0.05, **p < 0.01, two-tailed
288 Student's t tests against both controls. (F) Turning responses of flies where L1 and L3 were silenced together (golden
289 brown) and their specific Gal4 control (gray), color-coded according to ON edge luminance. The same five moving ON
290 edges of 100% contrast as in Figure 2A were shown. Responses of the other control *UAS-shi^{is}/+* to these stimuli have
291 been included in Figure 1C. (G) Peak velocities quantified for each of the five edges during the motion period, also
292 including the control *UAS-shi^{is}/+*, **p < 0.01, two-tailed Student's t tests against both controls. (H) Relationship of the
293 peak velocities with luminance, quantified as slopes of the linear fits to the data in (G). Slopes from the L3-silenced flies
294 (green, dashed) responding to the same stimuli (Figure 3C) are included again for comparison. Fitting was done for
295 individual flies. Sample sizes are n = 10 (*UAS-shi^{is}/+and L1,L3>>shi^{is}*) and n = 7 (*L1^{c2025}-Gal4/+;L3⁰⁵⁹⁵-Gal4/+*). (I)
296 Efficiency of the L1 and L3 behavioral rescue, calculated for each edge luminance as $(\text{rescue} - \text{ort}^- \text{ control}) / (\text{ort}^+ \text{ control} - \text{ort}^- \text{ control})$. *p<0.05, **p < 0.01, permutation test with 1000 permutations over the L1 *ort* rescue and L3 *ort*
297 rescue flies. (J) Summary schematic. The ON pathway in addition to the OFF pathway receives a prominent input from
298 L3. Like the OFF pathway, the ON pathway drives contrast constant behavior. Traces and plots show mean ± SEM.
299

300

301 **The contrast-sensitive L2 provides input to the ON-pathway**

302 Besides L1 and L3, the remaining input downstream of photoreceptors is the contrast-sensitive
303 L2 neuron, which provides strong inputs to OFF-pathway neurons (Takemura et al., 2013). To
304 explore the possibility of L2 also being an ON pathway input, we silenced L2 outputs either
305 individually or together with L1. L2-silenced flies showed only slightly reduced turning to all ON
306 edges as compared to controls (Figure 5A,B) similarly to silencing L1 alone (Figure 3A,B).
307 However, when L1 and L2 were silenced together, fly turning responses were fully disrupted
308 across conditions (Figure 5C,D). Moreover, these flies did not turn to other ON contrasts steps
309 either (Supp. Figure 2). This shows that L2, together with L1, is required for ON behavioral
310 responses across different contrasts and luminances. Altogether, L1, L2 and L3 are all ON-
311 pathway inputs.



312

313 **Figure 5: The contrast-sensitive L2 provides input to the ON-pathway.** (A) Turning responses of flies where L2
 314 was silenced (purple) and their specific Gal4 control (gray), color-coded according to 100% contrast ON edge at five
 315 different luminances. Sample sizes are n = 9 ($L2^{21Dhh}>>shilts$) and n = 6 ($L2^{21Dhh}-Gal4/+$). (B) Peak velocities quantified
 316 for each of the five edges during the motion period, *p < 0.05, two-tailed Student's t tests against both controls. (C)
 317 Turning responses of flies where L1 and L2 were silenced together (brown) and their specific Gal4 control (gray), color-
 318 coded according to ON edge luminance. Sample sizes are n = 9 ($L1_{c2025},L2^{21Dhh}>>shilts$) and n = 8 ($L1_{c2025}-Gal4/+;L2^{21Dhh}-$
 319 $Gal4/+$). (D) Peak velocities quantified for each of the five edges during the motion period, ***p < 0.001, two-tailed
 320 Student's t tests against both controls. Traces and plots show mean \pm SEM.

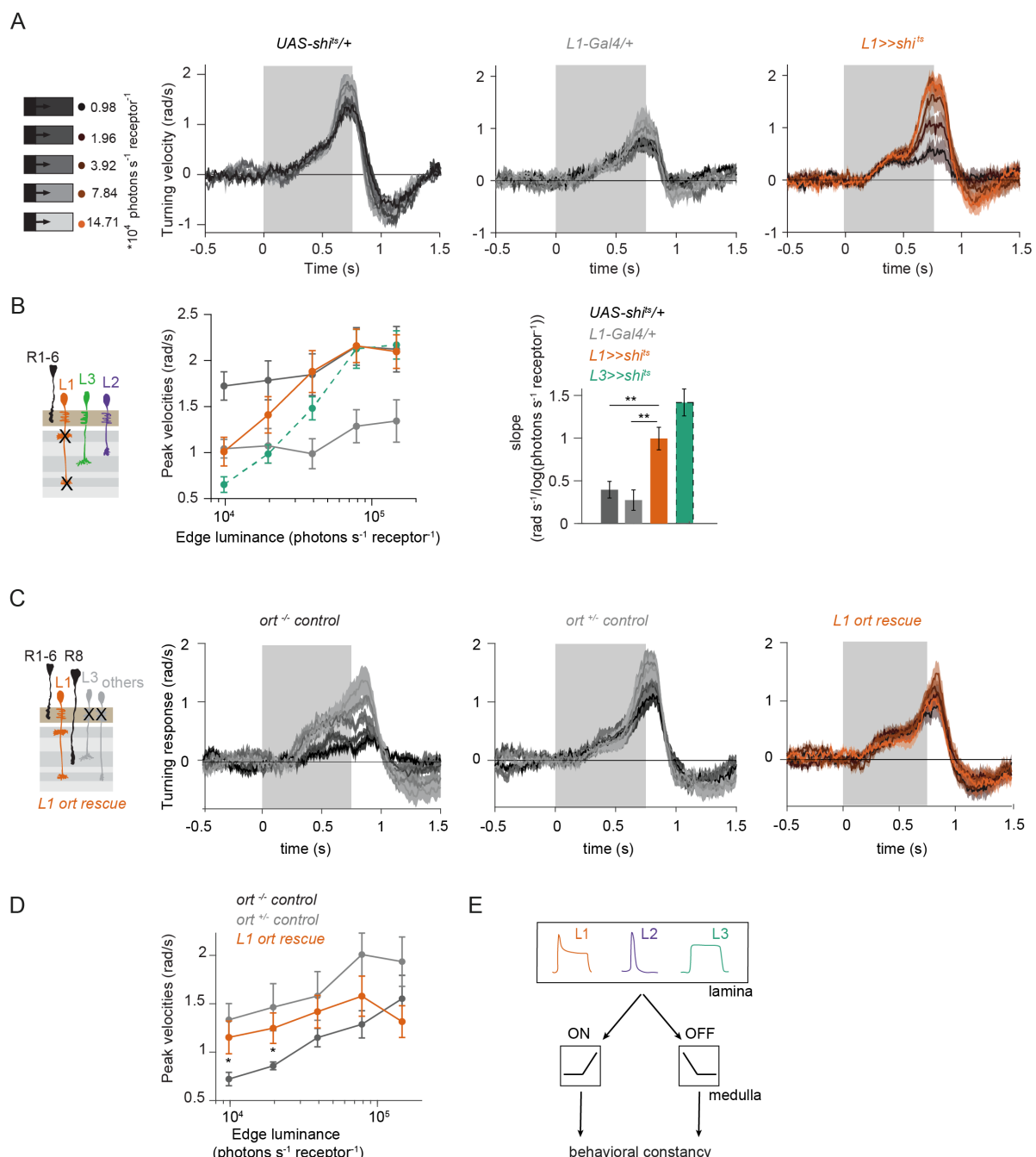
321

322 L1 is also an OFF pathway input

323

324 Given that three lamina neuron inputs encode visual stimuli differently and that all of them convey
 325 information to the ON-pathway, we next asked if L1 could also contribute to OFF-pathway
 326 function. To test this, we silenced L1 neurons while showing moving OFF edges, all of -100%
 327 contrast, and moving across five different background luminances. Control flies turned similarly
 328 under all conditions, showing lumiance-invariant responses (Figure 6A). Previous work showed
 329 that L3 is required to achieve lumiance invariance by scaling behavioral responses when
 330 background luminance turned dark (Ketkar et al., 2020). Similarly, when L1 was silenced,
 331 behavioral responses were no longer invariant across luminance, but flies turned less to -100%
 332 contrast at low luminance as compared to high luminance (Figure 6A,B). Underestimation of the
 333 dim OFF stimuli by L1-silenced flies was not as strong as by L3-silenced flies (Ketkar et al., 2020),
 334 again highlighting the specialized role of L3 in dim light (Figure 6B). These data demonstrate that
 335 L1 luminance inputs are required for lumiance-invariant OFF behavior. Since L1 carries both
 336 contrast and luminance information, it could be also sufficient to drive OFF behavior. To test this,
 337 we measured behavioral responses to OFF edges in L1 ort rescue flies. Heterozygous *ort* controls

338 showed turning responses to -100% OFF edges at five different luminances (Figure 6C). As
339 described previously (Ketkar et al., 2020), *ort* null mutants were not completely blind to this OFF-
340 edge motion stimulus and responded especially at high luminance but very little at low
341 luminances. L1 *ort* rescue flies responded similarly to positive controls, rescuing OFF edges at
342 low luminances (Figure 6D). Therefore, L1 is even sufficient to guide OFF behavior under the
343 same conditions that were previously described for L3 (Ketkar et al., 2020). Taken together, these
344 findings reveal that the lamina neurons L1 and L3 provide behaviorally relevant but differentially
345 encoded luminance information to both ON and OFF pathways. In sum, our data uncover L1, L2
346 and L3 as important inputs for both ON and the OFF pathways, relevant for visually guided
347 behaviors across luminances (Figure 6E).



348
349
350
351
352
353
354
355
356
357
358
359
360

Figure 6: The L1 luminance signal is required and sufficient for OFF behavior. (A) Turning responses of L1-silenced flies (orange) and the controls (gray) to five OFF edges moving onto different backgrounds. (B) Peak velocities quantified for each of the five edges during the motion period, also including the peak velocities of L3-silenced flies (green dashed, re-quantified from the data in (Ketkar et al., 2020)). Shown next to it is the relationship of the peak velocities with luminance, quantified as slopes of the linear fits to the data. ** $p < 0.01$, two-tailed Student's t tests against both controls (not significant against the $L3>>shi^ts$ slopes). Sample sizes are $n = 7$ ($L1-Gal4/+$) and $n = 10$ for other genotypes. (C) Schematics of the L1 ort rescue genotypes followed by its turning responses to the moving OFF edges. (D) Peak turning velocities of L1 ort rescue flies and the respective controls; * $p < 0.05$, two-tailed Student's t tests against both controls. Sample sizes are $n = 11$ flies ($ort^{-/-}$ control) and $n = 10$ for other genotypes. The gray box region in (A) and (C) indicates motion duration. (E) Summary schematic. Lamina neurons L1-L3 distribute different visual features necessary for both ON and OFF pathways to guide contrast-constant behavior. Traces and plots show mean \pm SEM.

361 **Discussion**

362 The present study establishes that contrast and luminance are basic visual features that interact
363 with both ON and OFF pathways. In both pathways, the interaction between these features
364 enables stable visual behaviors across changing conditions. The lamina neurons L1, L2 and L3
365 act as the circuit elements segregating both contrast and luminance information. Behavioral
366 experiments show that luminance information is required for contrast constancy in both ON and
367 OFF behaviors. While L1 and L3 provide contrast inputs to both ON and OFF pathways, L1 also
368 encodes luminance, together with L3. Whereas L3 activity non-linearly increases with decreasing
369 luminance, L1 shows a linear relationship with luminance. Luminance information from both
370 neurons is differently used in ON and OFF pathways. Thus, L1, L2 and L3 are not ON or OFF
371 pathways specific inputs, but they instead distribute the two most basic visual features, contrast
372 and luminance, across pathways to enable behaviorally relevant computations.

373

374 **Contrast constancy is a common feature of ON and OFF visual pathways, but with
375 distinct implementations**

376 Our work shows that visual behaviors guided by both ON and OFF pathways are luminance
377 invariant. Similarly, luminance invariance has been shown in human perception of both ON and
378 OFF contrasts, and in neural responses in cat LGN (Burkhardt et al., 1984; Mante et al., 2005).
379 This argues that luminance invariance is a common feature of all visual systems, which is
380 ethologically relevant for any species that relies on visual information for its survival in changing
381 visual environments. Changing visual environments impose a common challenge onto the
382 encoding of both ON and OFF contrasts, namely the contrasts are underestimated in sudden dim
383 light. The L1 contrast-sensitive responses reflect such underestimation. Thus, both ON and OFF
384 visual pathways would require a luminance-based correction to achieve luminance invariance,
385 and such correction would in turn rely on luminance-sensitive neuronal signals themselves. We
386 now confirm this hypothesis for both ON and OFF pathways. Specifically, luminance information
387 from both L1 and L3 are required for luminance-invariant visual behaviors. However, the impact
388 of the two neurons on behavior is pathway dependent. In the OFF pathway, losing either L1 or L3
389 function leads to a strong deviation from luminance invariance, such that the dim light stimuli are
390 underestimated. On the contrary, ON motion-driven behavior only strongly deviates from
391 invariance if both L1 and L3 neuron types are not functional. Furthermore, L2 neurons, which
392 were formerly thought to be OFF pathway inputs, contribute contrast-sensitive information to ON
393 behavior (Clark et al., 2011; Joesch et al., 2010; Silies et al., 2013). Notably, ON and OFF contrast
394 constancy is not achieved symmetrically at every processing stage. For example, in the vertebrate
395 retina, ON RGCs encode a mixture of luminance-invariant and absolute (i.e. luminance-
396 dependent) contrast, whereas OFF RGCs encode predominantly absolute contrast (Idrees and
397 Münch, 2020). Thus, asymmetrical implementation of contrast-corrective mechanisms can be
398 common across visual systems, too.

399

400 **All lamina neurons are inputs to both ON and OFF pathways**

401 L1, L2 and L3 all show different contrast and luminance sensitivities. These distinct neuronal
402 properties are then differentially utilized across ON and OFF pathways. How does this fit with the
403 established notion that L1 is an input to the ON and L2 and L3 are inputs to OFF pathways? The
404 luminance-varying stimuli sets used here were able to pull out lamina neuron contributions that
405 were not obvious with simpler stimuli. For example, our data show that L1 and L2 provide
406 redundant contrast input to the ON pathway at 100% contrast and varying luminance. However,
407 L1 is still strictly required for ON responses if different contrasts are mixed. This is consistent with
408 a more complex ON pathway input architecture and hints at a role for the L1 pathway in contrast
409 adaptation. Interestingly, Mi1, an important post-synaptic partner of L1, shows an almost
410 instantaneous and strong contrast adaptation (Matulis et al., 2020).
411 All three lamina neuron types hyperpolarize to light onset and depolarize to light offset and are
412 not contrast selective themselves. Contrast selectivity emerges downstream of these neurons:
413 known post-synaptic partners of L1 acquire ON contrast selectivity due to inhibitory glutamatergic
414 synapses, whereas cholinergic L2 and L3 synapses retain OFF contrast selectivity (Molina-
415 Obando et al., 2019). While L3 was actually already suggested to be an ON pathway input based
416 on connectomics (Borst et al., 2020), other synaptic connections that link L1 to downstream OFF-
417 selective neurons, and link L2 and L3 to downstream ON-selective neurons still have to be
418 investigated in detail. However, it now becomes evident that a split in ON and OFF circuitry only
419 truly exists in downstream medulla neurons and direction-selective cells. The luminance and
420 contrast features encoded differently in L1, L2 and L3 lamina neurons are shared by both
421 pathways. Importantly, the distinct features that are passed on by the specific inputs downstream
422 of photoreceptors guide distinct behavioral roles.
423

424 **L1 and L3 convey luminance information to multiple pathways**

425 Behavioral experiments in combination with genetic manipulations show that both L1 and L3
426 neurons provide luminance information to achieve luminance-invariant behaviors. This
427 functional data is consistent with anatomical predictions suggesting a role for L3 in the ON
428 pathway based on synaptic contacts with ON-selective neurons (Takemura et al., 2013). L3 had
429 mostly been considered an OFF pathway neuron because the OFF pathway neuron Tm9 receives
430 its strongest input from L3 (Fisher et al., 2015; Shinomiya et al., 2014; Takemura et al., 2013).
431 Remarkably, L3 itself actually makes most synaptic connections with the ON-pathway neuron
432 Mi9. Further synapses of L3 with the ON-selective Mi1 neuron are similar in number to those with
433 Tm9 (Takemura et al., 2013). Finally, L3 can potentially also convey information to the chromatic
434 pathway, as Tm20 is its second strongest postsynaptic connection (Lin et al., 2016). There, L3
435 luminance sensitivity might play a relevant role in achieving color constancy, i.e., color recognition
436 irrespective of illumination conditions. Altogether, anatomical and functional data indicate that it
437 is time to redefine L3 as part of a luminance-encoding system rather than a mere OFF-pathway
438 input.

439 A role of L1 beyond the ON pathway was less obvious based on anatomical data but is supported
440 by functional connectivity studies showing that Tm9 properties rely in part on L1 input (Fisher et
441 al., 2015), and that Tm9 together with other OFF pathway interneurons displays contrast-
442 opponent receptive fields, adding evidence to the presence of ON information in the OFF pathway
443 (Ramos-Traslosheros and Silies, 2021). Connectomics data did not identify any known OFF-

444 pathway neurons postsynaptic to L1 and presynaptic to the OFF-motion selective neuron T5
445 (Takemura et al., 2013). L1 must therefore connect to the OFF pathway via interneurons. Among
446 the strongest postsynaptic partners of L1 are the GABAergic interneurons C2 and C3 that connect
447 to the OFF pathway (Takemura et al., 2013). Intercolumnar neurons downstream of L1, such as
448 Dm neurons (Nern et al., 2015), could further carry information to OFF-selective neurons, likely
449 through disinhibition from ON-selective inputs. In the vertebrate retina, intercolumnar amacrine
450 cells mediate interaction between ON and OFF bipolar cells, which has been shown to extend the
451 operating range of the OFF pathway (Manookin et al., 2008; Odermatt et al., 2012). Altogether,
452 strategies appear to be shared across animals in which type of interneurons help to convey
453 relevant features from one pathway to the other.

454

455 **Neurons postsynaptic to photoreceptors encode contrast and luminance differently**

456 Despite being postsynaptic to the same photoreceptor input, all lamina neurons respond
457 differently to light stimuli. L1 was previously considered the ON pathway sibling of the contrast-
458 sensitive L2, both with regard to its temporal filtering properties and at the transcriptome level
459 (Clark et al., 2011; Tan et al., 2015). However, L1 calcium signals show a transient and a
460 sustained response component, which are contrast- and luminance-sensitive, respectively.
461 Compared to photoreceptors, which also carry both contrast and luminance components, L1 still
462 amplifies the contrast signals received from the photoreceptors, since its transient component is
463 more pronounced than the one seen in the photoreceptor calcium traces (Gür et al., 2020). In
464 other insect species, different types of lamina neurons have also been distinguished based on
465 their physiological properties (Rusanen et al., 2018, 2017), although their specific luminance and
466 contrast sensitivities are yet unknown.

467 The two luminance-sensitive neurons L1 and L3 differ in their luminance-encoding properties.
468 L1's initial transient contrast response might reduce the operating range of the subsequent
469 luminance-sensitive baseline. L3's calcium responses show little adaptation and can utilize most
470 of its operating range to encode luminance. L3 seems to invest this wider operating range into
471 amplifying the darkest luminance values selectively and non-linearly. Thus, a predominantly
472 luminance-sensitive channel among LMCs may have evolved to selectively process stimuli in the
473 low luminance range. The different linear and non-linear properties of L1 and L3 might further
474 increase the dynamic range of luminance signaling (Odermatt et al., 2012). Together with the
475 pure contrast sensitivity of L2, the first-order interneurons in flies exhibit a wide range of
476 sensitivities with respect to contrast and luminance, and our data confirm the functional relevance
477 of the differential sensitivities. Diversifying feature encoding through distinct temporal properties
478 of first-order interneurons is a strategy employed to reliably handle wide luminance ranges.

479

480 **Similarities and differences of peripheral processing strategies across species**

481 In flies, three first-order interneurons feed contrast and luminance information into downstream
482 circuitry. In the mouse retina, more than 30 functionally distinct bipolar types show a spectrum of
483 temporal filter properties rather than a strict transient-sustained dichotomy, thus capturing a larger
484 diversity of temporal information in parallel channels (e.g., (Baden et al., 2016; Ichinose et al.,

485 2014; Odermatt et al., 2012)). Many bipolar cell types resemble L1, in that they have both
486 luminance and contrast signals in distinct response components (e.g., (Oesch and Diamond,
487 2011)). However, the degree of transience varies from cell type to cell type, and some
488 predominantly sustained bipolar cell types are also found, closely resembling the luminance-
489 sensitive L3 (e.g., (Awatramani and Slaughter, 2000; Ichinose et al., 2014)). Such diversification
490 of feature extraction at the periphery has been shown to be computationally advantageous,
491 especially when processing complex natural scenes (e.g. (Odermatt et al., 2012; Rieke and Rudd,
492 2009)). For example, during daylight, visual scenes can differ in intensity by 4 to 5 log units,
493 whereas electrical signals in cone photoreceptors reach a dynamic range of only two orders of
494 magnitude (Naka and Rushton, 1966; Normann and Perlman, 1979; Pouli et al., 2010; Schnapf
495 et al., 1990).

496 Although the vertebrate retina apparently has a much larger diversity of cell types to handle the
497 wide and complex statistics of the visual environments, there is only a single layer of processing
498 between photoreceptors and the first direction-selective cells, whereas in insects, there are two:
499 the lamina and the medulla. It seems as if the combined properties of bipolar cells are spread
500 across these two processing stages in the fly visual system: whereas some properties, such as
501 diversity of temporal filtering starts in LMCs, contrast selectivity only emerges in medulla neurons
502 and not directly in the first-order interneurons as it happens in bipolar cells. In both vertebrates
503 and invertebrates, the emergence of ON selectivity occurs through inhibitory glutamatergic
504 synapses, but whereas this happens at the photoreceptor-to-bipolar cell synapse in vertebrates,
505 it happens one synapse further down between lamina and medulla neurons in flies (Masu et al.,
506 1995; Molina-Obando et al., 2019). Taken together, LMCs and downstream medulla neurons
507 combined appear to be the functional equivalents of vertebrate bipolar cell layers. Given the size
508 limitations of the fly visual system to encode the same complex environment effectively, one
509 benefit of this configuration with an extra layer could be that it allows more combinations.
510 Furthermore, the photoreceptor-to-lamina synapse in the fly superposition eye already serves to
511 spatially pool information from different photoreceptors (Braitenberg, 1967; Clandinin and
512 Zipursky, 2002; Kirschfeld, 1967). In both visual systems, diversifying distinct information across
513 several neurons could serve as a strategy to reliably respond to contrast when luminance
514 conditions vary.

515

516 **Methods**

517

518 **Experimental model**

519 All flies were raised at 25 °C and 65 % humidity on standard molasses-based fly food while being
520 subjected to a 12:12h light-dark cycle. Two-photon experiments were conducted at room
521 temperature (20 °C) and behavioral experiments at 34 °C. Female flies 2-4 days after eclosion
522 were used for all experimental purposes. Lamina neuron driver lines used for genetic silencing
523 and *ort* rescue experiments were *L3⁰⁵⁹⁵-Gal4* (Silies et al., 2013), *L2^{21Dhh}-Gal4* and *L1^{c202a}-Gal4*
524 (Rister et al., 2007), and *UAS-shi^{ts}*, *ort¹,ninaE¹* and *Df(3R)BSC809* were from BDSC (# 44222,
525 1946 and 27380). Since the *ort¹* mutant chromosomes also carries a mutation in *ninaE¹*
526 (*Drosophila rhodopsin1*), we used the *ort¹* mutation in trans to a deficiency that uncovers the *ort*
527 but not the *ninaE* locus. *UAS-ort* was first described in (Hong et al., 2006). For imaging
528 experiments, GCaMP6f (BDSC #42747) was expressed using *L1^{c202a}-Gal4*, *L2^{21Dhh}-Gal4* (Rister
529 et al., 2007), and *L3^{MH56}-Gal4* (Timofeev et al., 2012). Detailed genotypes are given in Table 1.

530 Table 1.: Genotypes used in this study.

Name	Genotype	Figure
Imaging		
<i>L1>>GCaMP6f</i>	<i>w+; L1^{c202a}-Gal4 / +; UAS-GCaMP6f / +</i>	Fig 1, 2
<i>L2>>GCaMP6f</i>	<i>w+; UAS-GCaMP6f / +; L2^{21Dhh}-Gal4 / +</i>	Fig 2
<i>L3>>GCaMP6f</i>	<i>w+; L3^{MH56}-Gal4 / +; UAS-GCaMP6f / +</i>	Fig 2
Behavior		
<i>UAS-shibire^{ts} control</i>	<i>w+; + / +; UAS-shi^{ts} / +</i>	Fig 2, 3,4, 5, 6, S1, S2
<i>L3-Gal4 control</i>	<i>w+; + / +; L3⁰⁵⁹⁵-Gal4 / +</i>	Fig 4
<i>L3 silencing</i>	<i>w+; + / +; L3⁰⁵⁹⁵-Gal4 /UAS- shi^{ts}</i>	Fig 4
<i>L1-Gal4 control</i>	<i>w+; L1^{c202a}-Gal4 / +; + /+</i>	Fig 3, 6, S1
<i>L1 silencing</i>	<i>w+; L1^{c202a}-Gal4 / +; + /UAS- shi^{ts}</i>	Fig 3, 6, S1
<i>L1-Gal4, L3-Gal4 control</i>	<i>w+; L1^{c202a}-Gal4 / +; L3⁰⁵⁹⁵-Gal4 /+</i>	Fig 4
<i>L1, L3 silencing</i>	<i>w+; L1^{c202a}-Gal4 / +; L3⁰⁵⁹⁵-Gal4 /UAS- shi^{ts}</i>	Fig 4
<i>ort mutant</i>	<i>w+; UAS-ort / +; ort¹,ninaE¹ / Df(3R)BSC809</i>	Fig 3, 4, 6
<i>L3 ort +/- control</i>	<i>w+; + / +; L3⁰⁵⁹⁵-Gal4, ort¹, ninaE¹ / +</i>	Fig 4
<i>L3 ort rescue</i>	<i>w+; UAS-ort / +; L3⁰⁵⁹⁵-Gal4, ort¹,ninaE¹ / Df(3R)BSC809</i>	Fig 4

L1 ort +/- control	<i>w+; L1^{c202a}-Gal4 / +, ort¹, ninaE¹ / +</i>	Fig 3, 6
L1 ort rescue	<i>w+; UAS-ort / +; L1[c202a]; ort¹,ninaE¹ / Df(3R)BSC809</i>	Fig 3, 6
L2-Gal4 control	<i>w+; + / +; L2^{21Dhh}-Gal4 / +</i>	Fig 5,S2
L2 silencing	<i>w+; + / +; L2^{21Dhh}-Gal4 /UAS- shi^{ts}</i>	Fig 5, S2
L1-Gal4, L2-Gal4 control	<i>w+; L1^{c202a}-Gal4 / +; L2^{21Dhh}-Gal4 / +</i>	Fig 5, S2
L1, L2 silencing	<i>w+; L1^{c202a}-Gal4 / +; L2^{21Dhh}-Gal4 /UAS- shi^{ts}</i>	Fig 5, S2

531

532 **Behavioral experiments**

533 Behavioral experiments were performed as described in (Ketkar et al., 2020). In brief, all
534 experiments were conducted at 34 °C, a restrictive temperature for *shibire^{ts}* (Kitamoto, 2001).
535 Female flies were cold anesthetized and glued to the tip of a needle at their thorax using UV-
536 hardened Norland optical adhesive. A 3D micromanipulator positioned the fly above an air-
537 cushioned polyurethane ball (Kugel-Winnie, Bamberg, Germany), 6 mm in diameter, and located
538 at the center of a cylindrical LED arena that spanned 192° in azimuth and 80° in elevation (Reiser
539 and Dickinson, 2008). The LED panels arena (IO Rodeo, CA, USA) consisted of 570 nm LEDs
540 and was enclosed in a dark chamber. The pixel resolution was ~2° at the fly's elevation. Rotation
541 of the ball was sampled at 120 Hz with two wireless optical sensors (Logitech Anywhere MX 1,
542 Lausanne, Switzerland), positioned toward the center of the ball and at 90° to each other (setup
543 described in (Seelig et al., 2010). Custom written C#-code was used to acquire ball movement
544 data. MATLAB (Mathworks, MA, USA) was used to coordinate stimulus presentation and data
545 acquisition. Data for each stimulus sequence were acquired for 15-20 minutes, depending on the
546 number of distinct epochs in the sequence (see 'visual stimulation' for details).

547

548 **Visual stimulation for behavior**

549 The stimulation panels consist of green LEDs that can show 16 different, linearly spaced intensity
550 levels. To measure the presented luminance, candela/m² values were first measured from the
551 position of the fly using a LS-100 luminance meter (Konica Minolta, NJ, USA). Then, these values
552 were transformed to photons incidence per photoreceptor per second, following the procedure
553 described by (Dubs et al., 1981). The highest native LED luminance was approximately 11.77 *
554 10⁵ photons * s⁻¹ * photoreceptor⁻¹ (corresponding to a measured luminance of 51.34 cd/m²), and
555 the luminance meter read 0 candela/ m² when all LEDs were off. For all experiments, a 0.9 neutral

556 density filter foil (Lee filters) was placed in front of the panels, such that the highest LED level
557 corresponded to $14.71 \times 10^4 \text{ photons} \cdot \text{s}^{-1} \cdot \text{receptor}^{-1}$.

558 Fly behavior was measured in an open-loop paradigm where either ON or OFF edges were
559 presented. For every set of ON or OFF edges, each epoch was presented for around 60 to 80
560 trials. Each trial consisted of an initial static pattern (i.e., the first frame of the upcoming pattern)
561 shown for 500 ms followed by 750 ms of edge motion. Inter-trial intervals were 1s. All edges from
562 a set were randomly interleaved and presented in a mirror-symmetric fashion (moving to the right,
563 or to the left) to account for potential biases in individual flies or introduced when positioning on
564 the ball.

565 The ON edge stimuli comprised four edges, each covering 48° arena space. All ON edges moved
566 with the angular speed of 160°/s. Thus, within a 750 ms stimulus epoch, the edge motion repeated
567 thrice: After each repetition, the now bright arena was reset to the pre-motion lower LED level,
568 and the next repetition followed immediately, picking up from the positions where the edges
569 terminated in the first repetition. This way, each edge virtually moved continuously. The following
570 sets of ON edges were presented:

- 571 1. 100% contrast edges: Here, the edges were made of 5 different luminance values (i.e. five
572 unique epochs), moving on a complete dark background. Thus, the pre-motion LED level was
573 zero, and the edges assumed the intensities 7%, 14%, 27%, 53% or 100% of the highest LED
574 intensity (corresponding to the luminances: 0.98, 1.96, 3.92, 7.84 or $14.71 \times 10^4 \text{ photons} \cdot \text{s}^{-1} \cdot \text{receptor}^{-1}$ luminance). Thus, every epoch comprised 100% Michelson contrast. The inter-
575 trial interval consisted of a dark screen.
 - 576 2. Mixed-contrast edges – full range: The set comprised of seven distinct epochs, each with a
577 different Michelson contrast value (11%, 25%, 33%, 43%, 67%, 82% and 100%). Here, the
578 edge luminance was maintained constant at 67% of the highest LED intensity, across epochs,
579 and the background luminance varied. The inter-trial interval showed a uniformly lit screen
580 with luminance equivalent to the edge luminance.
 - 581 3. Mixed-contrast edges – low contrast range: The set comprised of four distinct epochs, with
582 contrasts from the range 9%, 18%, 27% and 36%. Here, edge luminances and background
583 luminances both varied: The edge luminances assumed the intensities 80%, 87%, 93% and
584 100% of the highest LED intensity, whereas the background intensities were 67%, 60%, 53%
585 and 47% of the highest LED intensity, respectively. The inter-trial interval consisted of a dark
586 screen.
- 587

588

589 For the experiments concerning OFF edges, a set of five OFF edges comprising 100% Weber
590 contrast was used as described in (Ketkar et al., 2020). Epoch consisted of a single OFF edge
591 presented at one of five different uniformly lit backgrounds. The edge luminance was always
592 ~zero, whereas the five different background luminances were 7%, 14%, 27%, 54% and 100% of
593 the highest LED intensity (corresponding to five different background luminances: 0.98, 1.96,
594 3.92, 7.84 or $14.71 \times 10^4 \text{ photons} \cdot \text{s}^{-1} \cdot \text{receptor}^{-1}$). The inter-trial interval consisted of a dark screen.

595

596

597 **Behavioral data analysis**

598 Fly turning behavior was defined as yaw velocities that were derived as described in (Seelig et
599 al., 2010), leading to a positive turn when flies turned in the direction of the stimulation and to a
600 negative turn in the opposite case. Turning elicited by the same epoch moving either to the right
601 or to the left were aggregated to compute the mean response of the fly to that epoch. Turning
602 responses are presented as angular velocities (rad/s) averaged across flies \pm SEM. Peak
603 velocities were calculated over the stimulus motion period (750ms), shifted by 100 ms to account
604 for a response delay, and relative to a baseline defined as the last 200 ms of the preceding inter-
605 stimulus intervals. For the moving edges of 100% contrast and varying luminance, relation
606 between peak velocities and luminance was assessed by fitting a straight line ($V =$
607 $a \cdot \log(\text{luminance}) + b$) to the peak velocities of individual flies and quantifying the mean slope (a)
608 \pm SEM across flies. When comparing the slopes computed for behavior and L1 physiology, the
609 two data types were first normalized for individual flies for behavior and individual regions of
610 interest (ROIs) for L1 physiology (Figure 1E). For the *ort* rescue experiments, rescue efficiency
611 was calculated at each stimulus luminance as

612
$$E_{\text{rescue}} = \frac{\text{rescue} - \text{control}^-}{\text{control}^+ - \text{control}^-}$$

613 where E_{rescue} is the fractional rescue efficiency, *rescue* is the mean peak velocity of the rescue
614 genotype such as L1 rescue, *control*⁻ is the mean peak velocity of the *ort* null mutant negative
615 control and *control*⁺ stands for the mean peak velocity of the positive heterozygous *ort*¹ control
616 (e.g., *L1-Gal4; ort*^{1/+}). Statistical significance of E_{rescue} differences was tested using a permutation
617 test. Specifically, flies of the genotypes L1 *ort* rescue and L3 *ort* rescue were shuffled 1000 times
618 and the difference between their rescue efficiencies was obtained each time. The difference
619 values so obtained gave a probability distribution that approximated a normal distribution. The
620 efficiency difference was considered significant when it corresponded to less than 5% probability
621 on both tails of the distribution.

622 Mean turning of flies as well as the slopes from control and experimental genotypes were normal
623 distributed as tested using a Kolmogorov-Smirnov test ($p > 0.05$). Two-tailed Student's t tests and
624 Bonferroni-Holm correction were performed between genotypes. Data points were considered
625 significantly different only when the experimental group significantly differed from both genetic
626 controls. Flies with a baseline forward walking speed of less than 2 mm/s were discarded from
627 the analysis. This resulted in rejection of approximately 25% of all flies.
628

629 **Two-photon imaging**

630 Female flies were anesthetized on ice before placing them onto a sheet of stainless-steel foil
631 bearing a hole that fit the thorax and head of the flies. Flies they were head fixated using UV-
632 sensitive glue (Bondic). The head of the fly was tilted downward, looking toward the stimulation
633 screen and their back of the head was exposed to the microscope objective. To optically access
634 the optic lobe, a small window was cut in the cuticle on the back of the head using sharp forceps.
635 During imaging, the brain was perfused with a carboxygenated saline-sugar imaging solution
636 composed of 103 mM NaCl, 3 mM KCl, 5 mM TES, 1 mM NaH₂PO₄, 4 mM MgCl₂, 1.5 mM

637 CaCl₂, 10 mM trehalose, 10 mM glucose, 7 mM sucrose, and 26 mM NaHCO₃. Dissections were
638 done in the same solution, but lacking calcium and sugars. The pH of the saline equilibrated near
639 7.3 when bubbled with 95% O₂ / 5% CO₂. The two-photon experiments for Figure 2 were
640 performed using a Bruker Investigator microscope (Bruker, Madison, WI, USA), equipped with a
641 25x/NA1.1 objective (Nikon, Minato, Japan). An excitation laser (Spectraphysics Insight DS+)
642 tuned to 920 nm was used to excite GCaMP6f, applying 5-15 mW of power at the sample. For
643 experiments in Figure 1, a Bruker Ultima microscope, equipped with a 20x/NA1.0 objective (Leica,
644 Jerusalem, Israel) was used. Here the excitation laser (YLMO-930 Menlo Systems, Martinsried,
645 Germany) had a fixed 930 nm wavelength, and a power of 5-15 mW was applied at the sample.
646 In both setups, emitted light was sent through a SP680 shortpass filter, a 560 lpxr dichroic filter
647 and a 525/70 emission filter. Data was acquired at a frame rate of ~10 to 15Hz and around 6–8x
648 optical zoom, using PrairieView software.

649

650 **Visual stimulation for imaging**

651 For the staircase stimuli and light flashes of different luminances, the visual stimuli were
652 generated by custom-written software using C++ and OpenGL and projected onto an 8cm x 8cm
653 rear projection screen placed anterior to the fly and covering 60° of the fly's visual system in
654 azimuth and 60° in elevation. These experiments were performed with the Bruker Investigator
655 microscope.

656 For ON-moving edges, the stimulus was generated by custom-written software using the Python
657 package PsychoPy (Peirce, 2008), and then projected onto a 9cm x 9cm rear projection screen
658 placed anterior to the fly at a 45° angle and covering 80° of the fly's visual system in azimuth and
659 80° in elevation. These experiments were performed with the Bruker Ultima microscope.

660 Both stimuli were projected using a LightCrafter (Texas Instruments, Dallas, TX, USA), updating
661 stimuli at a frame rate of 100 Hz. Before reaching the fly eye, stimuli were filtered by a 482/18
662 band pass filter and a ND1.0 neutral density filter (Thorlabs). The luminance values are measured
663 using the same procedure described above for the behavioral experiments. The maximum
664 luminance value measured at the fly position was 2.17×10^5 photons s⁻¹ photoreceptor⁻¹ for the
665 staircase and random luminance stimulation, and 2.4×10^5 photons s⁻¹ photoreceptor⁻¹ for the ON-
666 moving edge stimulation. The imaging and the visual stimulus presentation were synchronized as
667 described previously (Freifeld et al., 2013).

668

669 Staircase stimulation

670 The stimulus consisted of 10s full-field flashes of 5 different luminances (0, 0.25, 0.5, 0.75 and
671 1* of the maximal luminance I_{max}). The different luminance epochs were presented first in an
672 increasing order (from darkness to full brightness) then in a decreasing order (full brightness to
673 darkness). This sequence was repeated ~3-5 times.

674

675 Flashes of different luminances

676 The stimulus consisted of 10s full-field flashes of 5 different luminances (0, 0.25, 0.5, 0.75 and
677 1* of the maximal luminance I_{max}). The order between the flashes was pseudo-randomized and
678 the stimulus sequence was presented for ~300s.

679

680 **ON moving edges at different luminances**

681 Here, the edges were made of 6 different luminance values (corresponding to 0.16, 0.31, 0.62,
682 1.2, 1.8, 2.4 * 10^5 photons*s⁻¹*receptor⁻¹ luminance), moving on a dark background. The inter-
683 stimulus interval was 4 seconds of darkness.

684

685 **Two photon data analysis**

686 **Staircase stimulation and randomized flashes of different luminances**

687 Data processing was performed offline using MATLAB R2019a (The MathWorks Inc., Natick, MA).
688 To correct for motion artifacts, individual images were aligned to a reference image composed of
689 a maximum intensity projection of the first 30 frames. The average intensity for manually selected
690 ROIs was computed for each imaging frame and background subtracted to generate a time trace
691 of the response. All responses and visual stimuli were interpolated at 10 Hz and trial averaged.
692 Neural responses are shown as relative fluorescence intensity changes over time ($\Delta F/F_0$). To
693 calculate $\Delta F/F_0$, the mean of the whole trace was used as F_0 . In some recordings, a minority of
694 ROIs responded in opposite polarity (positively correlated with stimulus), as described previously
695 (Fisher et al., 2015). These ROIs have their receptive fields outside the stimulation screen (Fisher
696 et al., 2015; Freifeld et al., 2013). To discard these and other noisy ROIs, we only used ROIs that
697 were negatively correlated (Spearman's rank correlation coefficient) with the stimulus. Plateau
698 responses were calculated as the mean of the last 2 seconds within each luminance presentation.
699 In the randomized flashes of different luminances, plateau response values of the highest
700 luminance epoch were subtracted for each plateau response to get a comparable relationship
701 between each neuron for visualization (this leads to 0 plateau response for each neuron in the
702 highest luminance condition). Mutual information between luminance and response was
703 calculated according to (Ross, 2014). To characterize the distinct luminance-response
704 relationships of L1 and L3, the difference of Pearson correlation and Spearman's rank correlation
705 was used as a Non-linearity index. This value will reach zero if there is a strict linear relationship
706 between luminance and response.

707

708 **ON moving edges at different luminances**

709 Data processing was performed offline using Python 2.7 (Van Rossum 1995). Motion correction
710 was performed using the SIMA Python package's Hidden Markov Model based motion correction
711 algorithm (Kaifosh et al., 2014). The average intensity for manually selected ROIs was computed
712 for each imaging frame and background subtracted to generate a time trace of the response. To
713 calculate $\Delta F/F_0$, the mean of the whole trace was used as F_0 . The traces were then trial averaged.
714 Responses of ROIs for each epoch was calculated as the absolute difference between the mean

715 of the full darkness background epoch and the minimum of the ON edge presentation (minimum
716 values are chosen because L1 neurons respond to ON stimuli with hyperpolarization).

717

718 Statistics

719 Throughout the analysis procedure, mean of quantified variables were calculated first for all ROIs
720 within a fly, and then between flies. All statistical analysis was performed between flies. For
721 normally distributed data sets, a two-tailed Student *t* test for unpaired (independent) samples was
722 used. For other data sets, Wilcoxon rank-sum was used for statistical analysis. Normality was
723 tested using Lilliefors test ($p>0.05$). One way ANOVA was used followed by multiple comparisons
724 using the Bonferroni method for determining statistical significance between pairs of groups.

725

726

727 **Acknowledgments**

728

729 We thank members of the Silies lab for comments on the manuscript. We are grateful to Christine
730 Gündner, Simone Renner, and Jonas Chojetzki for excellent technical assistance.

731 This project has received funding from the European Research Council (ERC) under the
732 European Union's Horizon 2020 research and innovation program (grant agreement No 716512),
733 and from the German Research Foundation (DFG) through the Emmy-Noether program (SI
734 1991/1-1) and the collaborative research center 1080 "Neural homeostasis" (project C06) to MS,
735 as well as DFG grant MA 7804/2-1 to CM.

736

737

738 **Author contributions:**

739 Conceptualization: MK, BG, SMO and MS

740 Methodology: MK, BG, CM

741 Software: MK, BG, SMO

742 Investigation: MK, BG, SMO, MI

743 Visualization: MK, BG, SMO

744 Supervision: MS, CM

745 Writing—original draft: MK, SMO, MS

746 Writing—review & editing: all authors

747 Funding acquisition: MS

748

749

750 **Competing interest:**

751 The authors declare no competing interests.

752 **Bibliography**

- 753
- 754 Awatramani GB, Slaughter MM. 2000. Origin of Transient and Sustained Responses in
755 Ganglion Cells of the Retina. *J Neurosci* **20**:7087–7095. doi:10.1523/JNEUROSCI.20-
756 18-07087.2000
- 757 Baden T, Berens P, Franke K, Román Rosón M, Bethge M, Euler T. 2016. The functional
758 diversity of retinal ganglion cells in the mouse. *Nature* **529**:345–350.
759 doi:10.1038/nature16468
- 760 Behnia R, Clark DA, Carter AG, Clandinin TR, Desplan C. 2014. Processing properties of on
761 and off pathways for *Drosophila* motion detection. *Nature*. doi:10.1038/nature13427
- 762 Borst A, Haag J, Mauss AS. 2020. How fly neurons compute the direction of visual motion. *J
763 Comp Physiol A* **206**:109–124. doi:10.1007/s00359-019-01375-9
- 764 Braatenberg V. 1967. Patterns of projection in the visual system of the fly. I. Retina-lamina
765 projections. *Exp Brain Res* **3**:271–298. doi:10.1007/BF00235589
- 766 Burkhardt DA, Gottesman J, Kersten D, Legge GE. 1984. Symmetry and constancy in the
767 perception of negative and positive luminance contrast. *J Opt Soc Am A* **1**:309.
768 doi:10.1364/JOSAA.1.000309
- 769 Chichilnisky EJ, Kalmar RS. 2002. Functional Asymmetries in ON and OFF Ganglion Cells of
770 Primate Retina. *J Neurosci* **22**:2737–2747. doi:10.1523/JNEUROSCI.22-07-02737.2002
- 771 Clandinin TR, Zipursky SL. 2002. Making connections in the fly visual system. *Neuron* **35**:827–
772 841. doi:10.1016/S0896-6273(02)00876-0
- 773 Clark DA, Bursztyn L, Horowitz MA, Schnitzer MJ, Clandinin TR. 2011. Defining the
774 Computational Structure of the Motion Detector in *Drosophila*. *Neuron*.
775 doi:10.1016/j.neuron.2011.05.023
- 776 Clark DA, Demb JB. 2016. Parallel Computations in Insect and Mammalian Visual Motion
777 Processing. *Curr Biol* **26**:R1062–R1072. doi:10.1016/j.cub.2016.08.003
- 778 Clark DA, Fitzgerald JE, Ales JM, Gohl DM, Silies MA, Norcia AM, Clandinin TR. 2014. Flies
779 and humans share a motion estimation strategy that exploits natural scene statistics. *Nat
780 Neurosci* **17**:296–303. doi:10.1038/nn.3600
- 781 Dubs A, Laughlin SB, Srinivasan MV. 1981. Single photon signals in fly photoreceptors and first
782 order interneurones at behavioral threshold. *J Physiol* **317**:317–334.
783 doi:10.1113/jphysiol.1981.sp013827
- 784 Euler T, Haverkamp S, Schubert T, Baden T. 2014. Retinal bipolar cells: Elementary building
785 blocks of vision. *Nat Rev Neurosci* **15**:507–519. doi:10.1038/nrn3783
- 786 Fischbach KF, Dittrich APM. 1989. The optic lobe of *Drosophila melanogaster*. I. A Golgi
787 analysis of wild-type structure. *Cell Tissue Res*. doi:10.1007/BF00218858
- 788 Fisher YE, Leong JCS, Sporar K, Ketkar MD, Gohl DM, Clandinin TR, Silies M. 2015. A Class of
789 Visual Neurons with Wide-Field Properties Is Required for Local Motion Detection. *Curr
790 Biol*. doi:10.1016/j.cub.2015.11.018
- 791 Frazor RA, Geisler WS. 2006. Local luminance and contrast in natural images. *Vision Res*
792 **46**:1585–1598. doi:10.1016/j.visres.2005.06.038
- 793 Freifeld L, Clark DA, Schnitzer MJ, Horowitz MA, Clandinin TR. 2013. GABAergic Lateral
794 Interactions Tune the Early Stages of Visual Processing in *Drosophila*. *Neuron*.
795 doi:10.1016/j.neuron.2013.04.024
- 796 Gür B, Sporar K, Lopez-Behling A, Silies M. 2020. Distinct expression of potassium channels
797 regulates visual response properties of lamina neurons in *Drosophila melanogaster*. *J
798 Comp Physiol A Neuroethol Sens Neural Behav Physiol* **206**:273–287.
799 doi:10.1007/s00359-019-01385-7
- 800 Hong S-T, Bang S, Paik D, Kang J, Hwang S, Jeon K, Chun B, Hyun S, Lee Y, Kim J. 2006.
801 Histamine and Its Receptors Modulate Temperature-Preference Behaviors in
802 *Drosophila*. *J Neurosci* **26**:7245–7256. doi:10.1523/JNEUROSCI.5426-05.2006

- 803 Ichinose T, Fyk-Kolodziej B, Cohn J. 2014. Roles of ON Cone Bipolar Cell Subtypes in
804 Temporal Coding in the Mouse Retina. *J Neurosci* **34**:8761–8771.
805 doi:10.1523/JNEUROSCI.3965-13.2014
- 806 Ichinose T, Hellmer CB. 2016. Differential signalling and glutamate receptor compositions in the
807 OFF bipolar cell types in the mouse retina: Temporal coding in the retinal OFF bipolar
808 cells. *J Physiol* **594**:883–894. doi:10.1113/JP271458
- 809 Ichinose T, Lukasiewicz PD. 2007. Ambient Light Regulates Sodium Channel Activity to
810 Dynamically Control Retinal Signaling. *J Neurosci* **27**:4756–4764.
811 doi:10.1523/JNEUROSCI.0183-07.2007
- 812 Idrees S, Münch TA. 2020. Different contrast encoding in ON and OFF visual pathways
813 (preprint). Neuroscience. doi:10.1101/2020.11.25.398230
- 814 Jin J, Wang Y, Lashgari R, Swadlow HA, Alonso J-M. 2011. Faster Thalamocortical Processing
815 for Dark than Light Visual Targets. *J Neurosci* **31**:17471–17479.
816 doi:10.1523/JNEUROSCI.2456-11.2011
- 817 Joesch M, Plett J, Borst A, Reiff DF. 2008. Response Properties of Motion-Sensitive Visual
818 Interneurons in the Lobula Plate of *Drosophila melanogaster*. *Curr Biol* **18**:368–374.
819 doi:10.1016/j.cub.2008.02.022
- 820 Joesch M, Schnell B, Raghu SV, Reiff DF, Borst A. 2010. ON and off pathways in *Drosophila*
821 motion vision. *Nature*. doi:10.1038/nature09545
- 822 Kaifosh P, Zaremba JD, Danielson NB, Losonczy A. 2014. SIMA: Python software for analysis
823 of dynamic fluorescence imaging data, *Frontiers in Neuroinformatics*.
- 824 Ketkar MD, Sporar K, Gür B, Ramos-Traslosheros G, Seifert M, Silies M. 2020. Luminance
825 Information Is Required for the Accurate Estimation of Contrast in Rapidly Changing
826 Visual Contexts. *Curr Biol*. doi:10.1016/j.cub.2019.12.038
- 827 Kirschfeld K. 1967. Die projektion der optischen umwelt auf das raster der rhabdomere im
828 komplexauge von *Musca*. *Exp Brain Res* **3**:248–270. doi:10.1007/BF00235588
- 829 Kitamoto T. 2001. Conditional modification of behavior in *Drosophila* by targeted expression of a
830 temperature-sensitiveshibire allele in defined neurons. *J Neurobiol* **47**:81–92.
831 doi:10.1002/neu.1018
- 832 Laughlin SB, Hardie RC. 1978. Common strategies for light adaptation in the peripheral visual
833 systems of fly and dragonfly. *J Comp Physiol* **128**:319–340. doi:10.1007/BF00657606
- 834 Leonhardt A, Ammer G, Meier M, Serbe E, Bahl A, Borst A. 2016. Asymmetry of *Drosophila* on
835 and off motion detectors enhances real-world velocity estimation. *Nat Neurosci*.
836 doi:10.1038/nn.4262
- 837 Lin T-Y, Luo J, Shinomiya K, Ting C-Y, Lu Z, Meinertzhagen IA, Lee C-H. 2016. Mapping
838 chromatic pathways in the *Drosophila* visual system: Chromatic Visual Circuits in the
839 Fly's Lobula. *J Comp Neurol* **524**:213–227. doi:10.1002/cne.23857
- 840 Manookin MB, Beaudoin DL, Ernst ZR, Flagel LJ, Demb JB. 2008. Disinhibition Combines with
841 Excitation to Extend the Operating Range of the OFF Visual Pathway in Daylight. *J
842 Neurosci* **28**:4136–4150. doi:10.1523/JNEUROSCI.4274-07.2008
- 843 Mante V, Frazor RA, Bonin V, Geisler WS, Carandini M. 2005. Independence of luminance and
844 contrast in natural scenes and in the early visual system. *Nat Neurosci* **8**:1690–1697.
845 doi:10.1038/nn1556
- 846 Masu M, Iwakabe H, Tagawa Y, Miyoshi T, Yamashita M, Fukuda Y, Sasaki H, Hiroi K,
847 Nakamura Y, Shigemoto R. 1995. Specific deficit of the ON response in visual
848 transmission by targeted disruption of the mGluR6 gene. *Cell* **80**:757–765.
- 849 Matulis CA, Chen J, Gonzalez-Suarez AD, Behnia R, Clark DA. 2020. Heterogeneous Temporal
850 Contrast Adaptation in *Drosophila* Direction-Selective Circuits. *Curr Biol*.
851 doi:10.1016/j.cub.2019.11.077
- 852 Mauss AS, Vlasits A, Borst A, Feller M. 2017. Visual Circuits for Direction Selectivity.
853 doi:10.1146/annurev-neuro-072116

- 854 Meinertzhagen IA, O'Neil SD. 1991. Synaptic organization of columnar elements in the lamina
855 of the wild type in *Drosophila melanogaster*. *J Comp Neurol* **305**:232–263.
856 doi:10.1002/cne.903050206
- 857 Molina-Obando S, Vargas-Fique JF, Henning M, Gür B, Schladt M, Akhtar J, Berger TK, Silies
858 M. 2019. ON selectivity in the *Drosophila* visual system is a multisynaptic process
859 involving both glutamatergic and GABAergic inhibition. doi:10.7554/eLife.49373.001
- 860 Naka KI, Rushton WAH. 1966. S-potentials from luminosity units in the retina of fish
861 (Cyprinidae). *J Physiol* **185**:587–599. doi:10.1113/jphysiol.1966.sp008003
- 862 Nern A, Pfeiffer BD, Rubin GM. 2015. Optimized tools for multicolor stochastic labeling reveal
863 diverse stereotyped cell arrangements in the fly visual system. *Proc Natl Acad Sci*
864 **112**:E2967–E2976. doi:10.1073/pnas.1506763112
- 865 Normann RA, Perlman I. 1979. The effects of background illumination on the photoresponses of
866 red and green cones. *J Physiol* **286**:491–507. doi:10.1113/jphysiol.1979.sp012633
- 867 Normann RA, Werblin FS. 1974. Control of Retinal Sensitivity I . Light and Dark Adaptation of. *J*
868 *Gen Physiol* **63**:37–61. doi:10.1085/jgp.63.1.37
- 869 Odermatt B, Nikolaev A, Lagnado L. 2012. Encoding of Luminance and Contrast by Linear and
870 Nonlinear Synapses in the Retina. *Neuron* **73**:758–773.
871 doi:10.1016/j.neuron.2011.12.023
- 872 Oesch NW, Diamond JS. 2011. Ribbon synapses compute temporal contrast and encode
873 luminance in retinal rod bipolar cells. *Nat Neurosci* **14**:1555–1561. doi:10.1038/nn.2945
- 874 Peirce JW. 2008. Generating stimuli for neuroscience using PsychoPy. *Front Neuroinformatics*
875 **2**. doi:10.3389/neuro.11.010.2008
- 876 Pouli T, Cunningham D, Reinhard E. 2010. Statistical regularities in low and high dynamic range
877 imagesProceedings of the 7th Symposium on Applied Perception in Graphics and
878 Visualization - APGV '10. Presented at the the 7th Symposium. Los Angeles, California:
879 ACM Press. p. 9. doi:10.1145/1836248.1836250
- 880 Ramos-Traslosheros G, Silies M. 2021. The physiological basis for contrast opponency in
881 motion computation in *Drosophila*. *Nat Commun* **12**:1–16. doi:10.1038/s41467-021-
882 24986-w
- 883 Ratliff CP, Borghuis BG, Kao Y-H, Sterling P, Balasubramanian V. 2010. Retina is structured to
884 process an excess of darkness in natural scenes. *Proc Natl Acad Sci* **107**:17368–17373.
885 doi:10.1073/pnas.1005846107
- 886 Reiser MB, Dickinson MH. 2008. A modular display system for insect behavioral neuroscience.
887 *J Neurosci Methods* **167**:127–139. doi:10.1016/j.jneumeth.2007.07.019
- 888 Rieke F, Rudd ME. 2009. The Challenges Natural Images Pose for Visual Adaptation. *Neuron*
889 **64**:605–616. doi:10.1016/j.neuron.2009.11.028
- 890 Rister J, Pauls D, Schnell B, Ting CY, Lee CH, Sinakevitch I, Morante J, Strausfeld NJ, Ito K,
891 Heisenberg M. 2007. Dissection of the Peripheral Motion Channel in the Visual System
892 of *Drosophila melanogaster*. *Neuron* **56**:155–170. doi:10.1016/j.neuron.2007.09.014
- 893 Ross BC. 2014. Mutual information between discrete and continuous data sets. *PLoS ONE*
894 **9**:e87357–e87357. doi:10.1371/journal.pone.0087357
- 895 Ruderman DL. 1994. The statistics of natural images. *Netw Comput Neural Syst* **5**:517–548.
896 doi:10.1088/0954-898X_5_4_006
- 897 Rusanen J, Frolov R, Weckström M, Kinoshita M, Arikawa K. 2018. Non-linear amplification of
898 graded voltage signals in the first-order visual interneurons of the butterfly *Papilio*
899 *xuthus*. *J Exp Biol* **221**:jeb179085–jeb179085. doi:10.1242/jeb.179085
- 900 Rusanen J, Vähäkainu A, Weckström M, Arikawa K. 2017. Characterization of the first-order
901 visual interneurons in the visual system of the bumblebee (*Bombus terrestris*). *J Comp*
902 *Physiol A Neuroethol Sens Neural Behav Physiol* **203**:903–913. doi:10.1007/s00359-
903 017-1201-9

- 904 Schnapf JL, Nunn BJ, Meister M, Baylor DA. 1990. Visual transduction in cones of the monkey
905 *Macaca fascicularis*. *J Physiol* **427**:681–713. doi:10.1113/jphysiol.1990.sp018193
- 906 Seelig JD, Chiappe ME, Dutta A, Osborne JE, Reiser MB, Jayaraman V. 2010. Two-photon
907 calcium imaging from head-fixed *Drosophila* during optomotor walking behavior. *Nat
908 Methods* **7**:535–40. doi:10.1038/nmeth.1468
- 909 Serbe E, Meier M, Leonhardt A, Borst A. 2016. Comprehensive Characterization of the Major
910 Presynaptic Elements to the *Drosophila* OFF Motion Detector. *Neuron* **89**:829–841.
911 doi:10.1016/j.neuron.2016.01.006
- 912 Shapley R, Enroth-Cugell C. 1984. Chapter 9 Visual adaptation and retinal gain controls. *Prog
913 Retin Res* **3**:263–346. doi:10.1016/0278-4327(84)90011-7
- 914 Shinomiya K, Huang G, Lu Z, Parag T, Xu CS, Aniceto R, Ansari N, Cheatham N, Lauchie S,
915 Neace E, Ogundeyi O, Ordish C, Peel D, Shinomiya A, Smith C, Takemura S, Talebi I,
916 Rivlin PK, Nern A, Scheffer LK, Plaza SM, Meinertzhagen IA. 2019. Comparisons
917 between the ON- and OFF-edge motion pathways in the *Drosophila* brain. *eLife*
918 **8**:e40025. doi:10.7554/eLife.40025
- 919 Shinomiya K, Karuppudurai T, Lin TY, Lu Z, Lee CH, Meinertzhagen IA. 2014. Candidate neural
920 substrates for off-edge motion detection in *drosophila*. *Curr Biol*.
921 doi:10.1016/j.cub.2014.03.051
- 922 Silies M, Gohl DM, Clandinin TR. 2014. Motion-Detecting Circuits in Flies: Coming into View.
923 *Annu Rev Neurosci* **37**:307–327. doi:10.1146/annurev-neuro-071013-013931
- 924 Silies M, Gohl DM, Fisher YE, Freifeld L, Clark DA, Clandinin TR. 2013. Modular Use of
925 Peripheral Input Channels Tunes Motion-Detecting Circuitry. *Neuron*.
926 doi:10.1016/j.neuron.2013.04.029
- 927 Strother JA, Nern A, Reiser MB. 2014. Direct observation of on and off pathways in the
928 *drosophila* visual system. *Curr Biol*. doi:10.1016/j.cub.2014.03.017
- 929 Strother JA, Wu ST, Wong AM, Nern A, Rogers EM, Le JQ, Rubin GM, Reiser MB. 2017. The
930 Emergence of Directional Selectivity in the Visual Motion Pathway of *Drosophila*. *Neuron*
931 **94**:168–182.e10. doi:10.1016/j.neuron.2017.03.010
- 932 Takemura Shin-ya, Bharioke A, Lu Z, Nern A, Vitaladevuni S, Rivlin PK, Katz WT, Olbris DJ,
933 Plaza SM, Winston P, Zhao T, Horne JA, Fetter RD, Takemura Satoko, Blazek K, Chang
934 LA, Ogundeyi O, Saunders MA, Shapiro V, Sigmund C, Rubin GM, Scheffer LK,
935 Meinertzhagen IA, Chklovskii DB. 2013. A visual motion detection circuit suggested by
936 *Drosophila* connectomics. *Nature*. doi:10.1038/nature12450
- 937 Takemura Shin-ya, Xu CS, Lu Z, Rivlin PK, Parag T, Olbris DJ, Plaza S, Zhao T, Katz WT,
938 Umayam L, Weaver C, Hess HF, Horne JA, Nunez-Iglesias J, Aniceto R, Chang L-A,
939 Lauchie S, Nasca A, Ogundeyi O, Sigmund C, Takemura Satoko, Tran J, Langille C,
940 Lacheur KL, McLin S, Shinomiya A, Chklovskii DB, Meinertzhagen IA, Scheffer LK.
941 2015. Synaptic circuits and their variations within different columns in the visual system
942 of *Drosophila*. *Proc Natl Acad Sci* **112**:13711–13716. doi:10.1073/pnas.1509820112
- 943 Takemura SY, Nern A, Chklovskii DB, Scheffer LK, Rubin GM, Meinertzhagen IA. 2017. The
944 comprehensive connectome of a neural substrate for ‘ON’ motion detection in
945 *Drosophila*. *eLife*. doi:10.7554/eLife.24394
- 946 Tan L, Zhang KX, Pecot MY, Nagarkar-Jaiswal S, Lee PT, Takemura SY, McEwen JM, Nern A,
947 Xu S, Tadros W, Chen Z, Zinn K, Bellen HJ, Morey M, Zipursky SL. 2015. Ig Superfamily
948 Ligand and Receptor Pairs Expressed in Synaptic Partners in *Drosophila*. *Cell*
949 **163**:1756–1769. doi:10.1016/j.cell.2015.11.021
- 950 Timofeev K, Joly W, Hadjieconomou D, Salecker I. 2012. Localized netrins act as positional
951 cues to control layer-specific targeting of photoreceptor axons in *drosophila*. *Neuron*
952 **75**:80–93. doi:10.1016/j.neuron.2012.04.037
- 953 Yang HH, Clandinin TR. 2018. Elementary Motion Detection in *Drosophila* : Algorithms and
954 Mechanisms. *Annu Rev Vis Sci* **4**:143–163. doi:10.1146/annurev-vision-091517-034153

955 Yang HHH, St-Pierre F, Sun X, Ding X, Lin MZZ, Clandinin TRR. 2016. Subcellular Imaging of
956 Voltage and Calcium Signals Reveals Neural Processing In Vivo. *Cell* **166**:245–257.
957 doi:10.1016/j.cell.2016.05.031
958

959 **Supplementary figures**

960
961
962

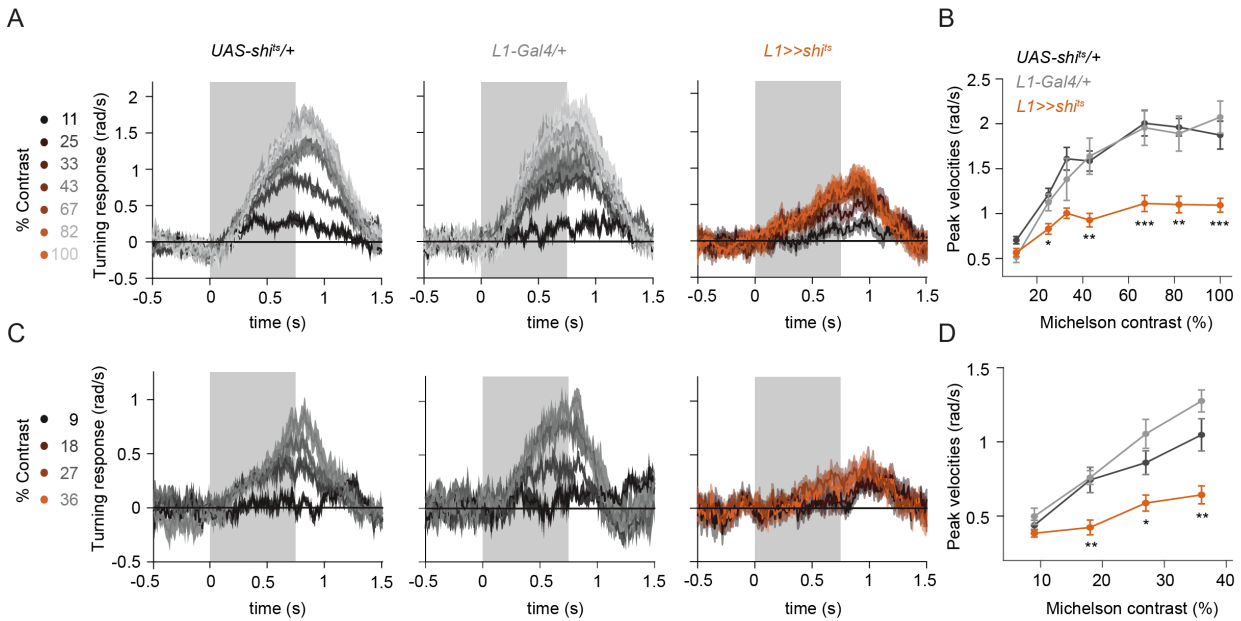


Figure S1: L1 is required for ON behavior across a range of contrasts. (A) Turning responses of the controls (gray) and L1-silenced flies (orange) in response to the moving ON edges of different contrasts, ranging from 11% to 100%. (B) Peak turning velocities quantified during the motion period, *p < 0.05, ***p < 0.01, ***p < 0.001, two-tailed Student's t tests against both controls. Sample sizes are n = 9 (UAS-shi^{ts}/+, L1^{c202a}>>shi^{ts}) and n = 5 (L1^{c202a}-Gal4/+). (C) Turning velocity time traces of the controls and L3-silenced flies in response to the moving ON edges of different contrasts, ranging from 9% to 36%. (D) Peak turning velocities quantified during the motion period, *p < 0.05, two-tailed Student's t tests against both controls. Sample sizes are n = 8 (UAS-shi^{ts}/+), n = 8 (L1^{c202a}>>shi^{ts}) and n = 5 (L1^{c202a}-Gal4/+). Traces and plots show mean ± SEM. The gray box region in (A) and (C) indicates motion duration.

963

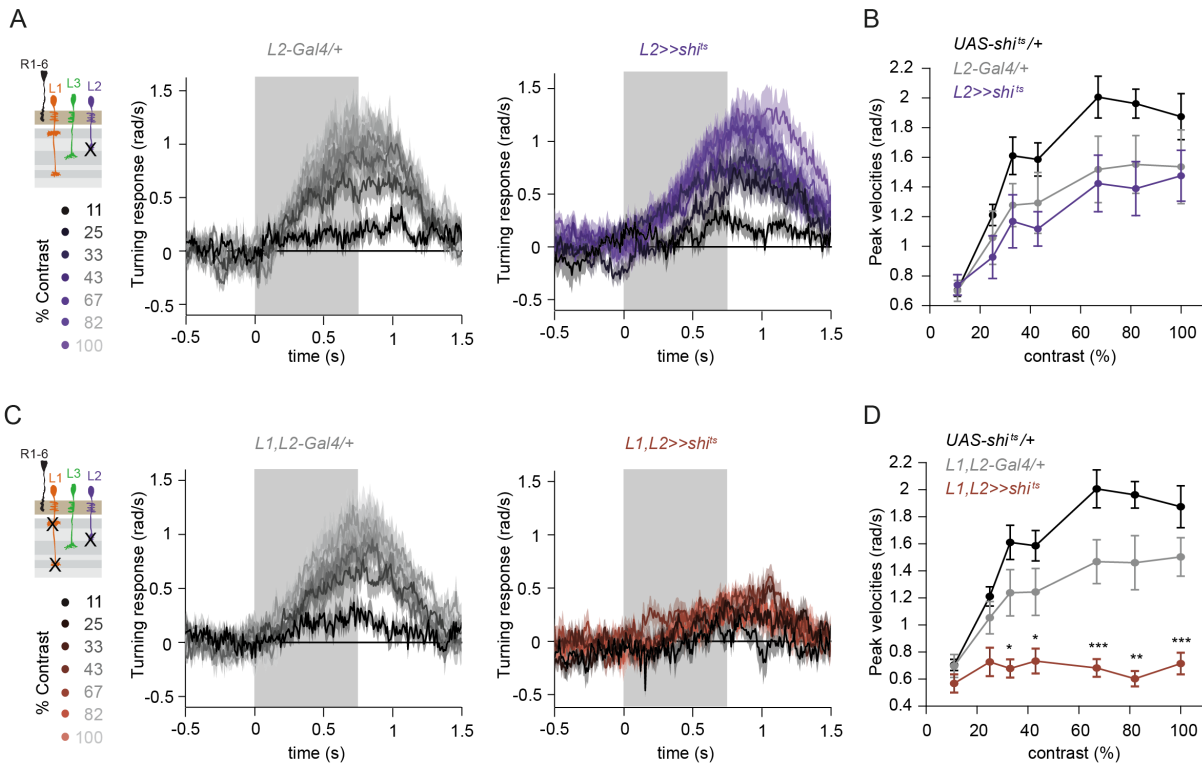


Figure S2: L1 and L2 together are required for ON behavior across a range of contrasts. (A) Turning velocity time traces of the Gal4 control (gray) and L2-silenced flies (purple) in response to the moving ON edges of different contrasts, ranging from 11% to 100%. (B) Peak turning velocities quantified during the motion period. Sample sizes are $n = 9$ (*UAS-shi^{ts}/+*), $n = 8$ ($L2^{21Dhh} >> shi^{ts}$) and $n = 8$ ($L2^{21Dhh}-Gal4/+$). (C) Turning velocity time traces of the Gal4 control and L1,L2-silenced flies (brown) in response to the moving ON edges of different contrasts, ranging from 11% to 100%. (D) Peak turning velocities quantified during the motion period, * $p < 0.05$, ** $p < 0.01$, *** $p < 0.001$, two-tailed Student's t tests against both controls. Sample sizes are $n = 9$ (*UAS-shi^{ts}/+*), $n = 8$ (*L1,L2 >> shi^{ts}*) and $n = 9$ (*L1,L2 -Gal4/+*). Traces and plots show mean \pm SEM. The gray box region in (A) and (C) indicates motion duration.